NTNU

Norwegian University of
Science and Technology

Low Short-Circuit Ratio Connection of Wind Power Plants

Anna Golieva

Wind Energy
Submission date: August 2015
Supervisor: Trond Toftevaag, ELKRAFT
Co-supervisor: Poul Sørensen, Danmarks Tekniske Universitet

Norwegian University of Science and Technology
Department of Electric Power Engineering

Low Short Circuit Ratio Connection of Wind Power Plants

Master of Science Thesis

Author:	Anna Golieva	
Supervisors:	Prof. Peter Palensky	TU Delft - Chairman
	Dr. Ir. Jose Luis Rueda Torres	TU Delft
	Prof. Trond Toftevaag	NTNU
	Prof. Poul Ejnar Sørensen	DTU
	Ömer Göksu	DTU
	John Bech	Siemens Wind Power

Abstract

Primary factor for the site selection during the planning process of the large modern wind farms is the wind climate, which is usually favorable at remote and offshore locations where the public grid is not particularly strong. Among the consequences of this solution is the necessity to connect wind farms to weak points of the grid and the necessity to reach this point by the means of long connection lines. All the mentioned factors result in a low short circuit ratio connection of wind farms becoming a frequent condition to deal with.

Wind turbine manufacturers and wind farm operators have already faced various engineering problems concerning the wind farms, operating in weak grids. One of them is inability to transfer the desired amount of the active power along the needed distance due to the lack of transmission capability. Besides that the system has to operate at the tip of its PV curve, which makes it vulnerable to voltage instability in case of sudden changes in a system, for instance a load connection or a short circuit. Furthermore, all the modern wind farms are using power electronic converter based drivetrain system, which has numerous advantages in terms of controllability but also demonstrates much lower short circuit current capabilities, compared to the previously used synchronous generator technology. That minimizes the modern wind turbines contribution to fault recovery, which in cases of severe faults might cause a wind power plant to violate the grid codes requirements, resulting in unfavorable consequences for the wind farm operator. Among the consequent instabilities, reported by the wind turbine manufacturers are the slow voltage recovery after system faults and oscillatory voltage instability in response to small disturbances.

A peculiarity of the previously held studies is that they are constrained by a range of case-dependent parameters, due to the fact that vast majority of the offered solutions propose the refinement of the turbine voltage controllers gains. The proposed solutions have demonstrated limited positive effect, however they are not universal, due to the fact that the voltage controllers are tuned on a case to case basis. Therefore this thesis carries out a systematic analysis of the nature of the occurring phenomenas instead of a case study solving. The investigated system is modeled, using the per-unitized conventional power system elements, with an emphasis on their mutual relations and not bound by the magnitudes. Therefore system behavior is not conditioned by any specific case peculiarities. On the contrary, the integral dependences are being tracked and the solutions are supplemented by the mathematical derivations, based on the fundamental power system laws.

Due to this approach the reason of the occurring instabilities has been detected, explained and resolved. Lack of transmission capabilities, shown by the simulations lays in the insufficient accuracy of the simplified power system modeling with the shunt capacitances neglected. The system, modeled with the shunt capacitances included does not possess the above-mentioned problems. Power system oscillations have been eliminated by means of controller tuning and insufficient voltage recovery has been overcome by means of partial reactive power compensation. The recommendations on modeling and control refinement are given, based on the derived dependences and tracked properties of the high impedance grid with high wind power penetration.

Acknowledgements

First of all I would like to thank DTU Wind Energy and my supervisors Poul Sørensen and Ömer Göksu for their help, inspiration and valuable guidances, provided throughout the entire span of the thesis work. My supervisor from Siemens Wind Power - John Bech for his time and comments, which make my work closer to the real-world requirements.

I would like to thank EWEM for making it possible for me to carry out the thesis work at DTU and I am extremely grateful to my supervisors from the degree-awarding universities, who have demonstrated outstanding flexibility, by accepting the challenging and unusual task to supervise a thesis student, located in another country. Thanks to Dr. Ir. Jose Rueda , Prof. Peter Palensky from TU Delft and Prof. Trond Toftevaag from NTNU.

I would like to express my great gratitude to my very first university, where I have started my engineering studies: Zaporizhzhya National Technical University and my home Electrical Technical Faculty and Electrical Apparatuses department. You gave me the passion for electrical engineering and confidence to aim for the best.

And thanks to everybody, who made me live normal life in spite of carrying out thesis work: Nick, my colleagues from the Risø office, my parents and Roskilde Festival - you have taught me to be in two different places at the same time and to find balance between work and life!

Contents

Nomenclature **v**

List of Figures **ix**

List of Tables **ix**

1 Introduction **1**

1.1 Analysis of Existing Literature 2

1.2 Scope of the Thesis and Scientific Approach 4

1.3 Research Objectives and Thesis Outline 6

2 Theoretical Background **9**

2.1 Full Scale Converter Wind Turbine 9

2.2 Grid Strength 10

2.3 Relevant Stability Definitions 12

3 System Modeling **15**

3.1 Simulation Tools 15

3.2 Simplified System Model 16

3.3 WT Model According to IEC Standards 18

3.4 Grid Codes Compliance 26

4 Simulations **29**

4.1 Simulated Cases 29

4.2 Modified System 35

4.3 Small-Signal Stability 40

4.4 Transient Stability 45

5 Effect of the SCR and X/R Ratio on the Controller Performance **53**

5.1 Control Refinement 53

5.2 SCR Influence 54

5.3 X/R Ratio Influence 58

6 Conclusions **61**

Appendices **67**

A Matlab Code for Per Unit Calculations 69

B Note on DIgSILENT PowerFactory 70

C Scientific Paper 73

Nomenclature

Abbreviations

CB	Circuit Breaker
CL	Closed Loop
DC	Direct Current
DFIG	Doubly-Fed Induction Generator
DIgSILENT	DIgital SImuLation of Electrical NeTworks
DSL	DigSilent Language
EMT	ElectroMagnetic Transients
GE	General Electric
HVAC	High Voltage Alternating Current
HVDC	High Voltage Direct Current
IEC	International Electrotechnical Commission
LOS	Loss of Synchronism
LVRT	Low Voltage Ride-Through
OL	Open Loop
PCC	Point of Common Coupling
PPM	Power Park Module
PWM	Pulse-Width Modulation
RMS	Root mean square (symmetrical steady-state)
SA	Synchronous Area
SCR	Short Circuit Ratio
SIL	Surge Impedance Loading
STATCOM	Static Synchronous Compensator
SVC	Static VAr Compe nsation
TSO	Transmission System Operator
UVRT	Undervoltage Ride-Through
VSC	Voltage Source Converter
VSWT	Variable Speed Wind Turbine
WPP	Wind Power Plant
WT	Wind Turbine
WTG	Wind Turbine Generator
XLPE	Cross-Linked PolyEthylene

Symbols

p_{WTref}	Wind turbine active power reference
X_{int}	Inductance between the wind turbine and point of common coupling
X_{th}	Inductive component of the Thevenin impedance
$\cos\phi$	Power factor
ΔU	Difference between the measured voltage and user defined voltage bias

δ	Voltage angle
$E_{S_{max}}$	Maximum limit of the sending end voltage
I_b	Current base
i_d	Direct axis current
i_q	Quadrature axis current
K_I	Integral gain
K_P	Proportional gain
P_{ramp}	Active power ramp rate
Q_{max}	Maximum WT reactive power
Q_{ref}	Wind turbine reactive power reference
r_{drop}	Resistive component of the voltage drop impedance
S_b	Power base
T_I	Integration time constant
t_0	Time when fault occurs
T_b	Torque base
t_{clear}	Fault clearing time
t_{rec}	Time within which the voltage returns to its steady-state limits
U_b	Voltage base
u_{ref0}	User defined voltage bias
x_{drop}	Inductive component of the voltage drop impedance
x_{WTref}	Wind turbine reactive power controller reference value
Z_b	Impedance base
Z_{th}	Thevenin impedance
1ϕ	Per phase value of a parameter
3ϕ	Three-phase value of a parameter
E_R	Receiving end voltage
E_S	Sending end voltage
X_T	Total impedance
Al	Aluminum
B	Succeptance
C	Capacitance
Cu	Copper
f	Frequency
I	Current
P	Active power
p.u.	per unit
Q	Reactive power
S	Apparent power
U	Voltage
X	Reactance

List of Figures

1.1 Typical wind farm grid connection 2

3.1 Simplified model of the system 16

3.2 Reduced model of the network 17

3.3 Block diagram for WPP reactive power controller 19

3.4 Block diagram for WT type 4b model 21

3.5 Block diagram for WT type 4b control model 22

3.6 Block diagram for Q control model 25

3.7 LVRT curve for the PPM type D 27

3.8 $U - Q/P_{max}$ profile of a Power Park Module at the Connection Point 28

4.1 PV-curves for strong and weak grids 31

4.2 PQ-curves for strong and weak grids 32

4.3 Pδ-curves for strong and weak grids 33

4.4 Limits of cables transmission capacity 37

4.5 Change of reactive power compensation along the active power ramp 38

4.6 PV and P-δ curves for the modified grid model 39

4.7 Eigenvalue plot for the original controller settings 40

4.8 dq currents and their references for strong and weak grids 42

4.9 Eigenvalue plot for the modified controller settings 43

4.10 Small disturbance application - load connection 44

4.11 Voltage response to a small disturbance with the original and the modified controllers 44

4.12 Enlarged oscillations of the system with modified controller 45

4.13 Fault location and tripping circuit breakers 46

4.14 Voltage profile at the PCC, as a result of SC fault at Z2 bus 47

4.15 Voltage difference between the PCC and Offshore bus during the fault 48

4.16 Injected reactive power 49

4.17 PCC voltage response to a fault, reduced Q compensation 50

4.18 PV and PQ curves for the final system model 51

4.19 Converter q-current, its limits and reference along the power ramp 51

5.1 Block diagram of the system transfer function 53

5.2 The designed system for the voltage dependence of SCR detecting 54

5.3 Voltage response to the stepwise increase in grid impedance 55

5.4 Interpolated voltage response to the increase in grid impedance 56

5.5 WT voltage as a function of the SCR at the WT bus 56

5.6 Error between the calculated and simulated values of the voltage 57

5.7 Block diagram of the modified system transfer function 58

5.8 Dependence of U_{WT} on SCR and X/R ratio 58

5.9 Maximum transferable active power as a function of X/R ratio 59

5.10 Powers for all the X/R cases 59

List of Tables

3.1 Two mass model 23

3.2 Generator control parameters 23

3.3 P control mode parameters 23

3.4 Q control mode parameters 24

3.5 Current limiter model 24

3.6 Admissible time periods and voltage range for the Nordic Synchronous Area 26

4.1 Investigated case parameters 29

4.2 Parameters of the various 132kV cables 36

4.3 Parameters of the modeled cable 36

4.4 Oscillation Parameters of the unstable poles 41

4.5 Oscillation Parameters of the poles after controller adjustment 43

4.6 Simulated events 46

1 | Introduction

There is a certain algorithm in wind farm planning process and it generally consists of the five subsequent cornerstones [1]:

- Wind resource
- Environmental impact
- Public acceptance
- Grid connection
- Project economy

It is clear, that wind resources assessment is the primary step of the wind farm planning process, as that is the factor, defining the annual energy production and thus the revenue. Consequently, grid connection is an issue, that is being discussed after the main features of the wind power plant (WPP) have been planned. Choosing the point of common coupling (PCC) based on voltage level alone is not satisfactory, therefore the deciding parameter is the grid 'strength' at the PCC [1], numerically expressed as the values of short circuit ratio (SCR). Earlier the SCR connection in a range of 2% - 20% used to be considered as a rule of thumb, because grid strength has an impact due to the following reasons [1]:

- Weak grid implies small conductors, resulting in low thermal limit of cables
- Injection of active and reactive power affects the voltage at the PCC greatly
- The stronger the grid, the smaller the voltage change
- The stronger the grid, the lower the effect of flicker and harmonic emissions

Nowadays tendency for lower SCR connection implementations are being observed. The reason behind this is that the primary factor for the WPP site selection are the quality of the wind resources, best of which are generally located at remote areas. Those areas are, generally, less populated, thus the electricity supplied to these areas is low and network does not need to be strong [1]. When it is about offshore wind farm connection, the total SCR, seen from the connection point, is further reduced by the connection cables. As it has been concluded by the European Wind Energy Association: over the years, offshore wind farms have moved further from shore. By the end of 2013, the average distance to shore from online wind farms was 29 km. Looking at projects under construction, consented or planned, this value is likely to increase [2].

1.1 Analysis of Existing Literature

The figure 1.1 demonstrates a typical WPP connection, which is going to be assumed throughout the thesis and corresponds to the topologies, used in the studied literature. It assumes that each turbine has its own turbine transformer, connected through the collector with the other radials to the park transformer (Main transformer at figure 1.1), being connected to the PCC by the high voltage (HV) lines. However, most of the research papers model WPP as an aggregated system, meaning a single turbine with the active power equal to the total power of the WPP. This assumption is valid in terms of the WPP-grid interaction studies, where the dynamics of individual turbines are not of studied, but the parameters of interests is the voltage at the PCC which is determined by the total power, injected by the turbines.

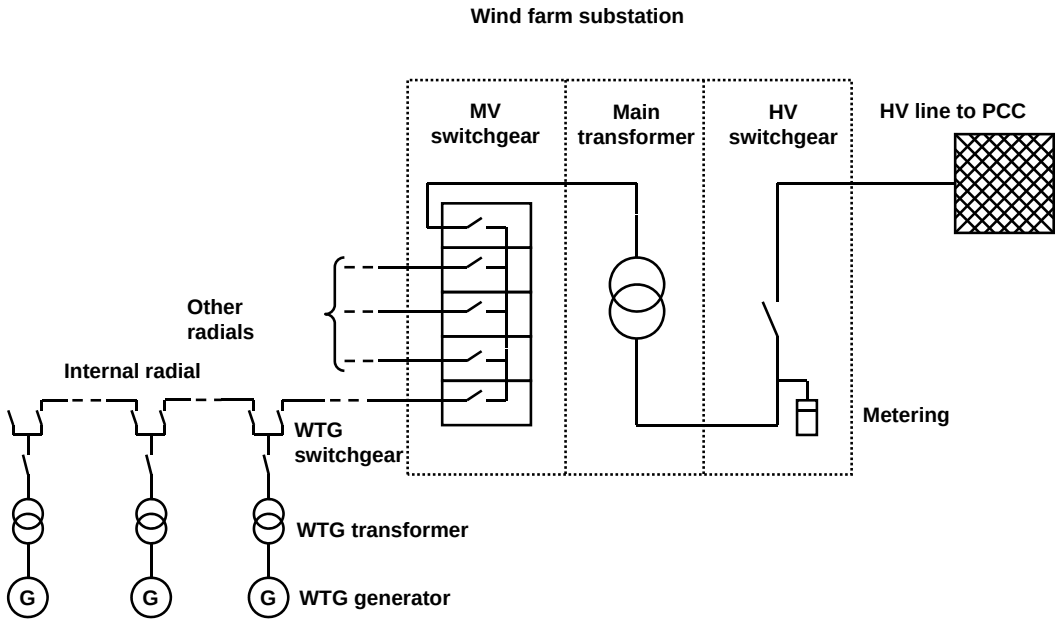

Figure 1.1: Typical wind farm grid connection [1]

Various research has been carried out on the topic within the wind turbine industry. However the majority of them are focused on specific cases. For example, [3] is carrying out dynamic simulations of the voltage disturbance response of the wind turbine generator (WTG) versus a conventional synchronous generator and presents relevant control design. However as it was stated by the authors, the model used was developed specifically for the General Electric (GE) 1.5 and 3.6 MW WTGs and the model is not intended to be used as a general purpose WTG [3]. Therefore, substantial difference in the developed controller performance may occur when applying to a WTG of a different manufacturer and capacity. Even though [4] presents extensive study of the voltage stability issues occurring when a wind park of large capacity being connected to a weak grid, the used grid model is fully represents a specific case of the ERCOT region grid in Texas.

Criteria of safe integration of large wind parks into weak grids have been studied in [5], whereas only induction machine based topologies have been investigated, namely types 1 (fixed speed squirrel cage induction generator) and 3 (variable speed wind turbine with doubly fed induction generator),

though the new generation wind turbines possess essentially different behavior due to presence of a full converter, which eliminates the typical synchronous machine response effect on the system. Although [6] mentions type 4 turbine (full converter), the study itself is focused on generator dynamic performance, which is not significantly relevant for the grid side of the full converter turbine type. An advanced control model against loss of synchronism (LOS) event have been developed in [7], which is, however, tuned for the specific 70MW WPP project and verified by the tests on downscaled 'Micro-WPP', which doesn't guarantee the effective results when being applied to a wind farm of a different topology.

Therefore, vast majority of the published papers lack generality, as they are, in a certain way case studies, which deal with the similar problems. Consequently the resulting solutions can rarely be applied to another WPP/network due to the absence of the derived dependences in conditions of system nonlinearity and controllers case-to-case tuning. Whereas this thesis work aims to carry out studies, applicable to the large variety of cases and to come up with the solutions, which any case study can benefit from.

However, certain case-independent solutions have been proposed from the industry and academia. In [8] it was discovered, that the fact, that WPP, unlike synchronous generator, is unable to increase the voltage in the weak grid during the fault. This is due to the fact, that while a synchronous generator is delivering high short circuit currents during faults, a WPP keeps its currents within nominal value. The ultimate conclusion states, that voltage recovery with the WTG operating with voltage support controller proportional gain $K_p = 2$ and power ramp $P_{ramp} = 20\%$ per second is even slower, than in a case with no generation. While some national grid codes, for example the German E.ON grid code [9], limits the minimum post-fault active power ramp to 20%. Therefore, as it has been concluded by the authors, the minimum requirements set in some grid codes for voltage support of WPPs are inadequate and do not result in a satisfactory voltage recovery in weak grids, as when reactive compensation is used to regulate the voltage in the weak grid, the voltage recovery with wind power installed appears to be worse than in the case with no generation [8]. However, the ultimate conclusion of [8] stated, that full-scale converter WPPs have the capability to provide a post-fault voltage support, which is comparable to the support by a synchronous generator of the same capacity, while in cases of low X/R ratios, this requires a coordinated injection of the WPP active and reactive current during the fault, in couple with voltage support without deadband after fault clearing [8]. That theory has been further developed in [8], which concluded, that the current injected by the WPP during the fault must have a $cos\phi$ dependency on the X/R ratio of the total network impedance as seen at the PCC, namely it must have an angle, opposite to the network impedance angle [8]. However, this strategy is not a specific solution for weak grids only, but rather a well-known method against prevention of LOS events in power systems [10].

The main concerns of the full converter concept are caused by the turbine behavior in response to grid faults, the issue being caused by low reactive power support capabilities. Even though the low voltage ride-through (LVRT) requirements demand that a wind turbine stays connected to the grid when a considerable voltage drop occurs, it is mostly resulting in WPP to maintain feeding active power into the grid, but the reactive power supply stays at the pre-fault level. Therefore it gives little contribution to the voltage recovery, compared to a conventional synchronous machine of the same capacity being connected to the same bus. The reason behind the difference is that a full converter, as it is typical for all power electronic appliances, possesses limited short circuit current capability. It is worth pointing out that in order to increase the reactive power supply necessary to recover the voltage, higher current injection is needed. That issues become particularly crucial on condition of weak grid, where $\frac{dV}{dQ}$ sensitivity is particularly high. It is known, that the converter current capabilities are limited, as

compared to the synchronous machine, conditioned by the importance of the converter protection against the high currents, therefore the limitations are to be set through the current limitation model in the converter control frame. It is common to design a power converter for a type 4 wind turbine with an overload capability of 10% above rated, therefore the maximum current value during the fault is 1.1 p.u. due to converter protection requirements [11]. The current is a complex current, i.e. $I_{max} = \sqrt{I_{real}^2 + I_{imag}^2}$. Therefore, in case the active current stays at the pre-fault value, say 1 p.u., there is only 0.45 p.u. capacity left for the reactive current, which is crucial for the voltage recovery.

Some proposed solutions from the industry, like [12] propose active power curtailment as a means of post-fault voltage recovery, especially for the weak grids. The relevance is conditioned by the fact, that there is a strong connection between the voltage at the node and the active power delivered to the node, which as well depends on an impedance of the utility grid - the higher the impedance of the utility grid the more rapidly the slope may decrease with increasing active power output [12]. However this solution is far from ideal, taking into account the primary purpose of the wind power plants, namely to deliver active power to the grid.

The first logical solution of the voltage instability seems to be refine control strategy, while certain problems arise there. The latest findings state that a weak grid is causing faster response of the closed-loop voltage control, which in its turn leads to the oscillatory response, and in some cases fast response can also lead to temporary overvoltages, up to high voltage collapse [4], also in numerous cases the so-called 'good' tuning in a weak grid results in faster response, but slows down recovery voltage and initiate voltage oscillations [4].

1.2 Scope of the Thesis and Scientific Approach

The analysis of the available literature has summed up the possible solutions, which are capable of solving the voltage instability problem:

- Grid reinforcement
- Application of flexible alternating current transmission system (FACTS)
- High voltage direct current (HVDC) connection
- Active power curtailment
- Injection of the current, having opposite angle to the line impedance angle
- Control refinement: WPP and WT controllers

Grid reinforcement is definitely the most expensive solution of the voltage stability problem, which is rarely being taken due to the fact, that the WPP operator is bearing the costs, which would make the project not feasible [1]. The vast majority of the research paper emphasize the importance of avoiding the necessity of the grid reinforcement.

HVDC connection is also an expensive solution, which is mostly used for very long transmission distances, where high voltage alternating current (HVAC) is no longer applicable [1]. Therefore, it

must be noted, that the further thesis only assumes the alternating current (AC) connected system. This decision is primarily conditioned by the fact, that so far, almost all offshore wind farms have used standard HVAC connections to bring their power ashore, but these are limited in length to 80–100 km, based on the active power capacity of the cable [14]. So far this value is the absolute maximum, it is known that even though all of the existing offshore wind farms operate with HVAC transmission system, the available technology limits their power transmission capability, however, three core cross-linked polyethylene (XLPE) cables with voltage rating up to 400 kV are under development which will allow power up to 800 MW to be transmitted at distances of 100 km [41]. However there are additional limitations, which do not depend solely on the material properties. For example, Danish Energy Agency and Energinet.dk estimate that foundation costs rise by 0.3 Mill. Euro/MW for every 10 meters of additional water depth, therefore at distances beyond typically 50 km from shore, the connection is done by an HVDC system instead of AC systems for technical reason [14]. The required installations lead to considerably higher costs. Therefore it was concluded, that for the distances up to 50 km the HVAC technology is the primary solution, wind farms located at greater distances offshore require HVDC connections [15], therefore only AC connection with the length of maximum 50 km will be considered in the thesis. Connection with cables, longer than 50 km is considered as a very specific case, introducing additional peculiarities, which are beyond the scope of the thesis.

FACTS devices is an expensive solution as well and the price depends on its capacity. Application of static synchronous compensator (STATCOM) has large amount of advantages due to the fact, that it operates based on pulse-width modulation (PWM) technology: operation down to zero SCR, black start capabilities, full active and reactive power control, etc. However, anything operating with PWM can behave as a STATCOM [16], including the Voltage Sourced Converter (VSC), used in wind turbines. They share the same drawbacks as well, for example STATCOM possesses the same limited short circuit current capability as wind turbine's VSC [4]. So in principle, the effect of STATCOM connected to a weak grid is in a large extent comparable with the effect of a WT converter, as have been noted by studied papers, for example [17]. STATCOM demonstrates faster voltage recovery after faults, even though it has reactive power dynamics comparable to VSC, however the principal reason for that is conditioned by the fact, that is the WTs active power injection causes extra voltage drop compared to a STATCOM [8]. Furthermore, the positive effect of STATCOM in case of dynamic events is highly dependent on its controllers tuning, therefore application of STATCOM requires the same controller tuning as the WT converter does. Therefore the application of STATCOM is not considered in this work due to high costs and absence of considerable advantages over VSC.

The first three of the proposed solutions do not meet the featured goal of the wind energy technologies development, which is known to be costs reduction. Even though the technologies have proven themselves to be effective from the engineering point of view, the high costs make them not feasible compared to the solutions, which do not require the additional costs. Therefore, among the discussed solutions, only control refinement is the one, which does not demand additional investments. As the cost reduction of wind energy is the main objective, claimed by the WT manufacturers and WPP operators, this thesis will concentrate on the WT controller influence on the grid connection stability of a WPP, connected to a weak grid. Injection of opposite angle current and active power curtailment are seen as measures within the control strategy refinement. The following chapters will concentrate on the system modeling as it was presented on figure 1.1, i.e. without additional power system elements, only by tuning the parameters of the WT controller, and without including the WPP controller, as it has been proven to be less effective and its dynamics might interfere with the dynamics of the WPP controller, distorting the observed phenomena.

1.3 Research Objectives and Thesis Outline

The vast majority of the studies, discussed in section 1.1 are representing the case studies, carried out by the manufacturers in order to solve the occurring problems during specific wind farms planning process. The models used for the study are manufacturer-specific ones, which are not available for the public [18], which in couple with the absence of the parametric settings make it impossible to implement the above-presented findings for the future research. Therefore the decision was made to use the generalized power system model for the low SCR connection studies, i.e. all the elements of the designed system are represented by its electrical characteristics and control strategies. This approach enables to determine the dependences and the nature of the occurring processes, therefore enabling a consistent solution and makes the system easy to reproduce for further studies.

The study particularly emphasizes the performance of the wind turbine controller in a weak grid. The used approach is convenient from the research point of view, as far as all the elements, interfering with the WT controller behavior are left out. The generalized system is represented by the conventional power system elements like voltage sources, resistances, reactances and capacitances, in couple with absence of WPP controller it makes it more evident to analyze the influence of the specific parameters on the overall performance.

The main measurable objective of this thesis is to model a connection of a WPP of 1 p.u. capacity to an extremely weak power system with SCR of 1 and to analyze its behavior. In order to accomplish this, the further steps will be taken:

- Create a simplified general model of the WPP-grid system
- Compare the WPP behavior on conditions of strong and weak grid. Analyze the reasons of the observed differences
- Select the optimal control modes for the grid connection of the WPP to a weak grid
- Ensure transmission of full WPP active power to the PCC
- Carry out small signal stability analysis of the system, with the further controllers refinement
- Perform the system transient stability check

Chapter 2 describes the peculiarities of the weak/low SCR grids high wind power penetration. Namely, it gives the extensive explanation of the weak grid nature, describes the essence of the voltage instability phenomena and controversial effects of the controller tuning. Additionally, the key features of the full-converter WPPs are explained with an emphasis on their performance in weak grids.

Chapter 3 gives an explanation of the state of art full-converter wind turbine parametric modeling approach in accordance with the latest International Electrotechnical Commission (IEC) standard, describes the numerical models peculiarities and gives an overview of the essential parameters, describes the process of the test system modeling in DIgSILENT PowerFactory, according to the IEC standard requirements, introducing relevant grid codes limitations.

Chapter 4 contains simulation results. Load flow study has been carried out in order to determine the limits of the active power transfer, demonstrating the difference of the WPP behavior in strong

and weak grids. The study has been supplemented by the small signal stability analysis, aiming to take into account the effect of the controller dynamics on the connection capabilities. investigate the fundamental difference between a WPP behavior in weak and strong grids, supplemented by the numerical derivations and the following updates of the model. Simulations of the updated model and the following optimization have been carried out.

Chapter 5 is devoted to elaboration of the plant transfer function, which would include the effect of the weak grid and that can be added into the conventional transfer function, which is used for the controllers tuning. That enables application of the existent transfer functions for the weak grids studies.

Chapter 6 summarizes the findings of the performed study, evaluation of the discovered phenomena and closes with recommendations for future research on the studied topic.

Appendix A contains Matlab code for the calculation of the per unit parameters of the designed system.

Appendix B contains the list and description of the elements, used for the system modeling in the DIgSILENT PowerFactory.

The attached paper *Full-Scale Converter Wind Turbines in Weak Grids* has been written within the scope of the course *Power Electronics in Future Power System* at the Norwegian University of Science and Technology and it has been carried out solely by the author of this thesis. The paper contains the preliminary literature study of the limited amount of parers, related to the topic and the performed load flow studies, investigating the influence of the line impedance magnitude versus X/R ratio onto the voltage deviations. The paper lays the groundwork for the succeeding dynamic simulations and determines the further scientific approach.

2 | Theoretical Background

This chapter addresses the most relevant theoretical issues, which are going to be considered in this thesis. It gives extensive overview of the terminology and specifics of the issue under consideration. The essence of the weak grid with high wind power penetration is being explained and supplemented by the mathematical dependencies. The peculiarities of the used wind turbine type are being explained with the comprehensive description of its generalized parameters. Additionally, relevant power system stability requirements and their features with respect to the turbine type used and the weak grid conditions are being briefly explained.

2.1 Full Scale Converter Wind Turbine

This section will give the extensive description of the state-of-art full converter WT drivetrain topology, corresponding to the IEC type 4. Even though DFIG (type 3) wind turbines are still being used, it is not considered as a progressive technology anymore due to considerably lower reliability compared to permanent magnet generators [19], the issue is becoming of greater importance when offshore application is considered. Therefore it was chosen to deal with general purpose wind turbine type 4 for the investigation of the problem.

The main features of the above-mentioned concept is the presence of full frequency converter, i.e. rating of the power converter in this wind turbine corresponds to the rated power of the generator. The converter completely decouples the generator from the network, enabling variable-speed operation [20]. It must be noted that the fundamental peculiarity of type 4 WTG due to the presence of a full converter, which decouples the generator from the grid, is that its behavior is no more similar to the one of a synchronous machine, i.e., commonly referred to issues of angle stability, field voltage and synchronism are no more relevant. Therefore the full-converter wind turbine is usually being modeled as a voltage source behind an impedance [3]. This decision has great influence on simulation results: in conventional modeling, when a wind turbine is modeled as a synchronous generator, the turbine interacts with the network through an internal angle, which does not meet the reality in case when full converter is used; the performance of the turbine is no more affected by the change of grid frequency [21].

The turbine is often represented as a voltage source behind an impedance as the fundamental frequency electrical dynamic performance of the WTG is completely dominated by the converter and the electrical behavior of the generator and converter is that of a current-regulated voltage source inverter [3]. Nevertheless the precise model should still possess certain properties of the conventional wind turbine model as its behavior is affected by factors, such as rotor inertia, blade pitching effects and intermittency due to effect of wind speed fluctuations. The latest require elaboration of the accurate wind model.

2.2 Grid Strength

The 'strength' of the grid is determined by its impedance and mechanical inertia, i.e. kinetic energy, stored in the rotating parts of the connected generators. Alternative representation, such as numerical value of the short circuit ratio, is nothing more, than a comparison of the system short circuit AC power and DC power injection at the specified bus. It must be noted, that SCR is not a strength indicator of an entire system, but a measure of the system strength at the specified point, therefore a system, consisting of numerous generators and transmission lines will have different value of the SCR at each specific bus. In this paper further use of the SCR value will be always referred with respect to the PCC. Summarizing, application of SCR as a measure of grid strength is understood as an accepted approximation [22].

However, distinction must be made between the terms 'Weak Grid' and 'Grid with low SCR'. The SCR of a bus is an indication of the strength of the bus, which is defined as the ability of the bus to maintain its voltage in response to reactive power variations. A system having high SCR will experience much less change in bus voltage than a network with low SCR [22]. As it has been stated in [4]: even though the SCR is calculated using steady state values, its value is a measure of how easily bus voltages are affected during dynamic system events.

First of all, the given studied situation refer to the general problems of grid with high wind power penetration. A system with wind power representing more, than 15% of total capacity is considered as a system with high penetration [5]. The wind power integration level is calculated as:

$$\rho = \frac{P_n}{S_{SC}} \tag{2.1}$$

where P_n is the nominal power of the wind farm and S_{SC} is the short circuit power of the grid. This parameter in certain way could also be referred to as an inverse of the short circuit ratio, which in its turn is expressed as:

$$SCR = \frac{S_{SC}}{P_n} \tag{2.2}$$

Though a certain clarification has to be emphasized: S_{SC} is a full power of a three-phase short circuit to ground, as seen at the PCC. This value has to be obtained theoretically, assuming grid to be modeled as a Thevenin voltage source, its voltage has to be divided by the Thevenin impedance:

$$S_{SC} = \frac{U_{PCC}^2}{Z_{th}} \tag{2.3}$$

In per unit (p.u.), taking into account that WPP capacity is 1 p.u. and assuming voltage at the PCC equal to 1 p.u., the expression is simplified to:

$$SCR_{PCC} = S_{SC} = {Z_{th}}^{-1} \tag{2.4}$$

Furthermore, the low SCR effect is aggravated by the large portion of shunt capacitances in the lines impedances. As it is known, that reactive power, produced by the capacitors is directly proportional to the voltage squared, therefore in case of a voltage dip the injected reactive power decreases quadrati-

cally, whereas higher reactive power injection is needed for the voltage recovery, therefore the capacitor brings a destabilizing effect in this case [22]. Due to that the effective short circuit ratio value is often used:

$$ESCR = \frac{S_{SC} - Q_c}{P_n} \tag{2.5}$$

where Q_c is the reactive power of all the shunt capacitances between a wind farm and a PCC.

In many cases, even when a wind park is being connected to a strong grid (i.e. low impedance grid or grid with high short circuit power) via long transmission lines, which in their turn have high impedance, the resulting SCR seen at the PCC is being reduced and its value is primary determined by the line length. Another issue of significant importance is the influence of the surge impedance loading (SIL) of the connecting line, as loaded below it SIL (which is the usual case for cables) the line is producing reactive power and when being loaded above SIL the line is absorbing reactive power.

$$P_{SIL} = \frac{U^2}{\sqrt{\frac{L}{C}}} \tag{2.6}$$

Therefore the nature of the connecting line have considerable effect on reactive power balance [24]:

1. Cables are considered to produce reactive power all the time, therefore in case of voltage drop the supplied reactive power decreases quadratically
2. On the contrary behavior of the overhead lines might change depending on the certain conditions. Voltage drop results in SIL decrease, which at certain conditions might lead to line being loaded above SIL, so the line, which is injecting reactive power in the system at normal condition might start absorbing reactive power during the fault and as a result have negative effect on voltage recovery.

Therefore, weak grids can be classified by the following types:

1. Grid with low SCR due to low voltage level at the PCC
2. Low SCR due to high grid impedance
3. Low SCR caused by connecting to low impedance grid through long cables
4. Grid internal fault resulting in increase of impedance and transient SCR drop

This thesis mainly investigates the phenomena, occurring in cases 2 and 3, because they have similar essence from the power system point of view - high value of impedance between the PCC and a grid make the system weak at the connection point. Even though a grid strength is expressed as a value of a SCR, it is highly dependent on a power system topology, which might be vulnerable to SCR drop in case, for example if one of the parallel lines is out due to fault. Therefore case 4 has been studied as well, within the scope of the contingency analysis.

2.3 Relevant Stability Definitions

Power system stability is generally defined as a property of power system, which enables it to remain in equilibrium under normal operating condition and to maintain a certain limit of equilibrium after being subjected to small and large disturbances [24]. Stability is generally subdivided into the fundamental groups:

- Rotor angle stability
- Voltage stability
- Frequency stability

Rotor angle stability lies in the ability of the interconnected synchronous generators to remain in synchronism [24], however due to the fact, that this thesis deals with the full-converter type wind turbine, which decouples the generator from the rest of the system, the rotor angle stability is not an issue.

Frequency stability refers to the ability of the power system to maintain steady frequency between generation and load, following a severe disturbance [25]. Though, as it has been mentioned in section 2.1, due to the presence of the full-scale frequency converter the issue becomes irrelevant.

Voltage stability is the subject of the study, as it is defined as the ability of a power system to maintain bus voltages at the acceptable limits under normal operating condition and after being subjected to disturbances [24]. Voltage instability occurs, when a disturbance is causing a a progressive and uncontrollable drop of voltage. A frequent phenomenon, referred to when referring to voltage instability is voltage collapse. Voltage collapse is defined as a process, by which the sequence of events, accompanying voltage instability leads to unacceptable (mostly - low) voltage profile in a significant part of the power system [24].

The essence of the voltage instability lies in power system inability to meet the reactive power demand, for example, a voltage drop occurs, when active and reactive power flow through the transmission network inductive reactance [24]. That situation, is in principle, describing what is happening in the weak grids, as they are characterized by high impedance, and as it is typical for the power systems, inductive component is prevailing.

The stability is as well classified, based on time duration as [24]:

- short-term or transient, 0 - 10 seconds
- mid-term, 10 seconds - few minutes
- long-term few minutes - 10's of minutes

The indicated times are roughly approximated as the classification is mainly based on the investigated processes. Mid-term and long-term stability are of interest within the scope of this thesis, as they are

associated with the power system responce to the severe upsets, which results in voltage excursions [24]. Long-term stability leaves out the inter-machine synchronizing power oscillations and power-angle stability issues, which are not relevant for the full-converter turbine type. id-term and long-term stability reflect consequences of the poor controllers tuning, which is of primary interest within the scope of the thesis.

3 | System Modeling

This chapter gives extensive explanation of the studied system modeling process. The initial system, representing the desired single-line diagram is going to be built, consisting solely of the PowerFactory library equipment and standard power system elements. In order to to make the essential studied element, namely the WT to behave like a real full-converter based WTG, a control frame will be enabled and set according to the IEC standard requirements. Some settings in the control frame are going to be kept the same as default ones, representing wind turbine essential electrical and mechanical characteristics, while the others are going to be changed in order to comply with the regulations of the grid codes.

3.1 Simulation Tools

The object of the research is the full-scale converter wind turbine, corresponding to the type 4 according to the IEC classification. The corresponding turbine model implementation in PowerFactory is going to be used. The main tool, which is going to be used throughout the thesis is time-domain simulations in DIgSILENT PowerFactory 15.2, namely balanced symmetrical steady-state (RMS) simulations. As it has been mentioned in the theoretical part, the thesis deals with long-term voltage stability, i.e. slow transient or quasi steady-state, therefore RMS simulations are used and not the electromagnetic transien (EMT) ones. The primary reason for it is that long-term stability deals with uniform system frequency, as demanded by the turbine models. The detailed description of the simulation tools, its functions and specification of the used elements are represented in Appendix B.

The RMS simulations is a favorable tool, because the models have been designed specifically for the dynamic simulations and they support all the features, which are required within the scope of this thesis, namely:

- change of system parameters
- stepwise variation of loads
- variations of controller setpoint
- circuit breakers tripping
- symmetrical short-circuit events

The objective of the study demands application of various power system analysis tools, large-disturbance voltage stability analysis to be carried out, in particular - study of the system behavior following system faults - such as transient voltage drops or similar contingencies. The study requires the examination of the nonlinear dynamic performance of the system over a time period, sufficient to capture all the

parameters of interest within their transient time limits, therefore long-term dynamic simulations are required for the analysis [24]. Long-term analysis is relevant for the stability problems due to insufficient active/reactive power reserve [24]. However, for the system modeling and derivation of connection capabilities it is necessary to carry out the load flow studies and the small-signal stability studies additionally. Even though the voltage stability has been previously defined as the ability of all the buses of a system to reach their acceptable level after the disturbance [24], however due to the grid codes requirements the parameter of interest is the voltage at the PCC, therefore the voltage stability is hereby assumed to be the ability of the voltage at the PCC to return to its specified limits after a disturbance.

3.2 Simplified System Model

The layout of the system designed for the preliminary studies is represented in figure 3.1.

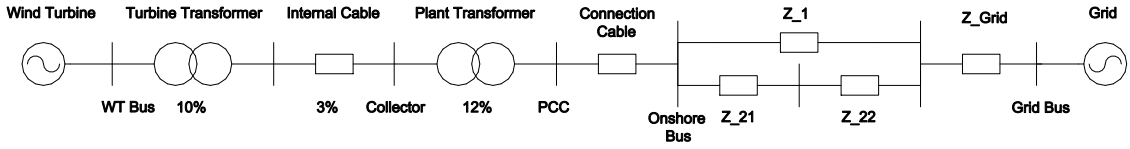

Figure 3.1: Simplified model of the system implemented in DIgSILENT Power Factory

Thevenin voltage source representation of the WT is performed by using the static generator (ElmGenstat) PowerFactory element, behaving as a controlled voltage source [26]. According to [44] the type 4A/B WTG is in the network represented via the static generator element and the initial settings for the load flow calculation and dynamic simulation are done in this element.The wind park is modeled as aggregated system, using the PowerFactory built-in aggregation function, i.e. parameters of a single turbine and a turbine transformer are set, in couple with number of parallel machines. The aggregation is a reasonable assumption, taking into account the fact, that impedance of a collector system is relatively small, compared to the transformer impedance [3].

Wind Turbine model according to IEC 61400-27-1 is used, type 4b turbine of 2MW active power, with 50 parallel machines, resulting in 100MW WPP capacity. Taking into account the fact, that the generation adequacy analysis is not being carried out and that the park controller is not attached, the turbines operate at the same conditions and their performance is identical. Therefore, there is no significance of the 2MW turbines application - the output of the aggregated system is equivalent to the single turbine model with 100MW active power output. The results of the simulations are, therefore, applicable to wind turbines of different capacity. The primary reason for the 2MW turbine model selection is that its realistic model according to IEC 61400-27-1 is included in PowerFactory library.

Turbine transformer, park transformer and internal cable are not specified in the standard and, therefore their specification was selected from the PowerFactory library, modeled in couple with IEC 61400-27-1 turbines. The turbine transformer has been modeled by means of the two-winding transformer element (ElmTr2) with the 10% impedance. The transformer impedance value can be seen as relatively high for the 2MW turbine, however, taking into account the general nature of the study it is justified by the fact, that for the 100MW WPP such value of transformer impedance can occur, for example, when the 6MW turbines are used in the WPP [27]. Therefore, taking into account the fact, that the aggregated parameters are of importance and not the single machines dynamics, it was decided to use

10% impedance, i.e. maximum realistic value for the turbine transformer [27], as far as using lower values might result in underestimating the total impedance value seen between the WT bus and the Grid Bus.

The external grid is modeled as a Thevenin voltage source, therefore Bus Grid is set as a slack bus. The parallel impedances, depicted on figure 3.1 are purposed to simulate the internal structure of the grid, i.e. including parallel lines and are going to be used for the succeeding contingency studies. For the sake of the case generalization all the elements on the right side of the PCC, i.e. the connecting line and the internal grid impedance, are represented by general impedances (ElmZpu). Therefore, the final model can be reduced to the equivalent representation:

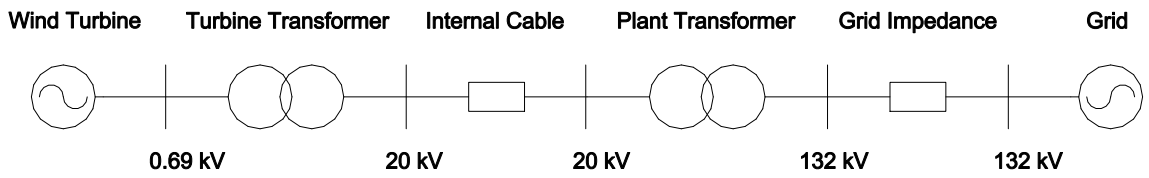

Figure 3.2: Reduced model of the network

The model was built in per unit in order to generalize it and to make it convenient to use the parameters of the IEC standard and for straightforward controllers tuning. Nominal value of WPP active power is used as per-unit base for all powers [18] i.e. $S_b = 100$MVA. This base has been assigned to all the general impedances elements, which are used in the model. There are three voltage levels at the system, corresponding to the three local voltage bases U_b: 0.69kV, 33kV and 132kV. Three corresponding base impedances have been calculated for the three zones according to the formula 3.1:

$$Z_b = \frac{{U_b}^2}{S_b} \tag{3.1}$$

The corresponding base impedances are: Z_b: 0.09Ω, 10.89Ω, 174.24Ω.

The values have been used in order to obtain the actual values of the equipment impedance, which are used by some elements in DIgSILENT PowerFactory, for example, by the cables. Furthermore, certain elements (for example, transformers) use the local p.u., therefore their values have to be converted into the global reference by the formula 3.2:

$$Z_{global} = Z_{local} \cdot \left(\frac{U_{local}}{U_{global}}\right)^2 \cdot \frac{S_{global}}{S_{local}} \tag{3.2}$$

The main parameter of interest is the utility voltage, which is the voltage at the PCC in p.u. The decision has practical reasoning, as in many countries influence on the steady-state voltage is the main design criteria for the grid connection of wind turbines, especially in distribution grids [21]. The precise calculation of the per unit values are attached in Appendix A.

3.3 WT Model According to IEC Standards

The WT is modeled as a controllable voltage source, therefore the behavior of this voltage source has to be defined by means of certain control frame. In order to make the voltage source represent the behavior of a WT, the DIgSILENT Simulation Language (DSL) control frame has to be assigned to the turbine. Therefore, it was decided to control the behavior of the turbine by means of the state-of-art wind turbine models according to IEC 61400-27. An integral part of this thesis work is application of the IEC 61400-27 standard concerning electrical simulation models for wind power generation. The models, specified by the standard are purposed for stability studies, and particularly for the short-term voltage stability phenomena investigation. The models are generic, i.e. it can represent different WTs/WPPs, by changing the model parameters. The standard is purposed to be used at educational institutions in particular, due to the fact, that manufacturers models are usually confidential [18]. The standard and thus the models are represented by a series of parametric modules, that eases the implementation of the desired turbine behavior in order to represent precisely the defined WT type.

According to [18] the models are designed specifically for the following studies:

- balanced short-circuits on the transmission grid (external to the wind power plant, including voltage recovery)
- grid frequency disturbances
- electromechanical modes of synchronous generator rotor oscillations
- reference value changes

The first and the last ones are relevant for this thesis.

The standard distinguishes between the four principal wind turbine types [18]:

- Type 1 uses asynchronous generators directly connected to the grid, without a power converter.
- Type 2 is similar to type 1, but the type 2 turbine is equipped with a variable rotor resistance and therefore uses a variable rotor resistance asynchronous generator.
- Type 3 uses a doubly fed induction generator, where the stator is directly connected to the grid and the rotor is connected through a back-to-back power converter.
- Type 4 are WTs connected to the grid through a full scale power converter.

Therefore, the desired turbine topology corresponds to the type 4 turbine according to the IEC specification. However, two type 4 models are specified by the IEC 61400-27 [28]:

- Type 4A without mechanical model
- Type 4B with mechanical model

That is due to the fact, that type 4 wind turbines without choppers inject post-fault power oscillations due to torsional oscillations, therefore the effect of torsional oscillations may be included using a two-mass mechanical model [28]. Type 4 wind turbines can normally be modeled neglecting the aerodynamic and mechanical parts of the turbine, because the torsional oscillations normally do not affect the power system stability. However, due to the fact, that the models are applied in couple with weak grid condition, where oscillatory stability is an issue, type 4B will be used in the study.

It has been previously mentioned, that the plant level voltage controller tuning possess very limited impact on voltage response in case of contingencies [4], and in couple with the fact that the WT has been modeled as an aggregated element it gives sufficient reasoning for using the WT-level controller only. The primary reason for WPP controller to be omitted, is mainly the fact, that if the WPP controller is omitted and no additional PWM-based devices are modeled, the influence of the WT controller on the system behavior will be easy to track, as the tracked signal will not be distorted by the other controllers. Stability of the WT controller will become the only concern and, therefore, this specific problem will be easier to detect and, therefore, to solve.

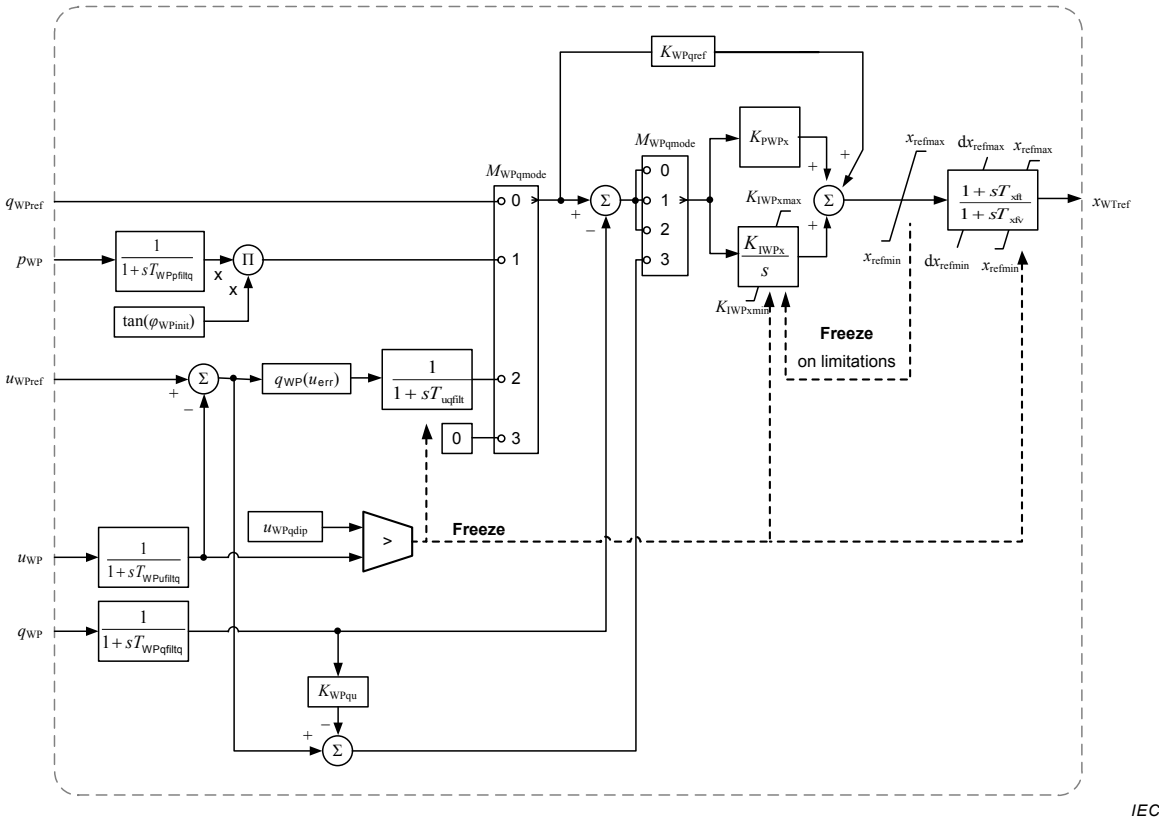

Figure 3.3: Block diagram for WPP reactive power controller [18]

However, neglecting the WPP controller requires certain adaptation of the WT model, because the WPP controller is responsible for voltage at the PCC, while the WT controller only sees the voltage at the WT bus, and the reference, needed to keep the PCC voltage at the desired level is being taken from the WPP controller. Therefore, an insight into the WPP controller structure has to be taken.

As it can be seen from the WPP reactive power controller, shown on figure 3.3, the only output of the plant controller is the reference value x_{WTref}, which, in its turn is the input parameter of the turbine Q controller, namely its reference value. In other words, the WPP controller is using the measurements from the PCC and compares them with the reference values, applies PI controller and outputs U/Q reference for the WT reactive power controller.

Therefore, in order to omit the WPP controller, the reference value x_{WTref} on figures 3.3 anf 3.6 has to be set as a constant value. In PowerFactory that value, when the plant controller is absent, is automatically taken from the load flow solution. Later this value can be changed by a parameter change event during the RMS simulations. However, the PCC voltage reference is not equal to the WT voltage reference, furthermore, their ratio is not a constant value, but it depends on the WT active and reactive power dispatch. Therefore, in order to control the voltage at the PCC, the WT voltage reference has to be converted into the PCC voltage reference, taking into account the WT operating point. Therefore, the 'voltage drop characteristic has been enabled in the reactive power control module, which is depicted on figure3.6. The block is purposed for calculation of the voltage at the remote point , intended to be used for example to control the voltage at the HV side of the transformer [18]. It is necessary to control the voltage at the PCC, however the voltage measurement input has to stay connected to the WT bus, due to cross-coupling as shown on the figure 3.6, the way to control voltage at the PCC is to set the series impedance drop parameters, and the voltage at the PCC will be calculated by the formula:

$$u = \sqrt{(u_{WT} - r_{drop} \cdot \frac{p_{WT}}{u_{WT}} - x_{drop} \cdot \frac{q_{WT}}{u_{WT}})^2 + (x_{drop} \cdot \frac{p_{WT}}{u_{WT}} - r_{drop} \cdot \frac{q_{WT}}{u_{WT}})^2} \tag{3.3}$$

where $r_{drop} = 0.03 p.u.$ is the series resistive component of the voltage drop impedance, and $x_{drop} = 0.25 p.u.$ is the series inductive component of the voltage drop impedance between the WT and the PCC, as can be seen from the figure 3.1 and listed in the table 3.4. However it must be noted, that this expression is only valid for the aggregated system, when the WPP is represented as a single WT. In case the system with the parallel turbines is modeled, the WPP controller must be included into the model.

The following three WT parameters can be used as references in the WT control models:

- Active power
- Reactive power
- Voltage reference

It can be seen from he block diagram of the WT type 4b, shown on figure 3.4, that there are two input parameters in the control module: p_{WTref} and x_{WTref}, the first one corresponds to the active power reference and the second one is using reactive power or voltage reference, depending on the reactive power control mode. x_{WTref} represents reactive power for the Q control and PF control modes, or ΔU (if $u_{ref0} = 0$) for the voltage control mode. As far as no park controller model is applied, this signal is initialized as a constant input [18], taken from the load flow.

There are three parameter categories in the IEC models:

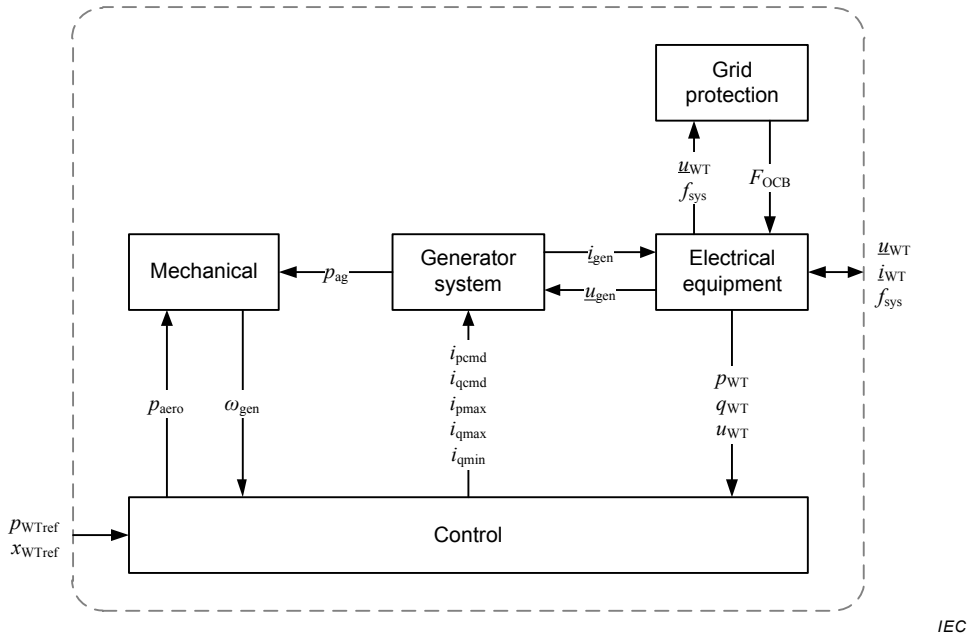

Figure 3.4: Block diagram for WT type 4b model [18]

1. Type parameters (typically mechanical and electrical parameters).
2. Project parameters (different for a specific WT type, depending on the project, typically control parameters are set according to specific grid codes)
3. Case parameters (vary depending on the operating point prior to the disturbance)

Type parameters are going to be set once and will remain unchanged throughout the work, while case parameters are going to be varied, based on the study case and project parameters will be modified in order to determine the optimal settings for the best performance and grid codes compliance. The only global parameters used are the electric frequency and simulation time step.

The general structure of the turbine model is represented on the figure 3.4 and the controller structure - on the figure 3.5. It must be noted, for the U control mode, only the right PI controller from the figure 3.6 is relevant (U control), while for Q control and PF control both PIs are used (Q control and U control). Some of the modules consist of Type parameters only, while rest of them include also Project and Case parameters.

PowerFactory implementation of the IEC models has been used, which is time domain positive sequence simulation models for dynamic simulations of short term stability of power systems have been used [18]. Tables 3.1-3.4 contain the default settings of the PowerFactory model of the WT type 4b. The default settings have been used for the preliminary simulations and will be updated throughout the work in order to achieve the improved performance of the turbine on condition of the weak grid connection. The PowerFactory implementation model of the type 4b turbine consists of the following modules:

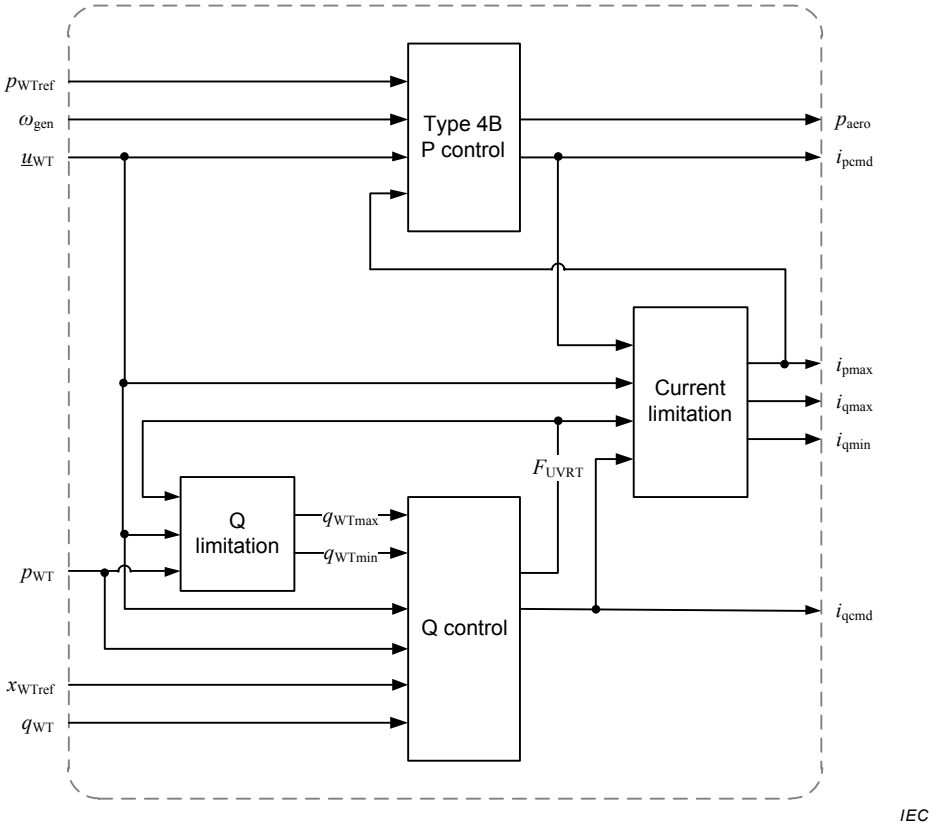

Figure 3.5: Block diagram for WT type 4b control model [18]

1. Two mass model
2. Type 4 generator set model
3. P control model type 4B
4. Q control model
5. Current limitation model
6. Constant Q limitation model or QP and QU limitation model
7. Grid protection model

It must be noted, that the Q limitation module is only relevant for Q control and PF control modes, while for the U control mode the reactive power limitation is carried out through the q-current limitation in the current limitation module.

The parameters from the table 3.1 represent the mechanical characteristics of the turbine, and, therefore, cannot be changed for the sake of performance optimization. They stay constant throughout the

Table 3.1: Two mass model

Name	Value	Unit	Category
Inertia constant of wind turbine rotor	5	s	Type
Inertia constant of generator	0.7	s	Type
Drive train damping	1	T_b/w_b	Type
Drive train stiffness	80	T_b	Type

Table 3.2: Generator control parameters

Name	Value	Unit	Category
Time constant	0.01	s	Type
Minimum reactive current ramp rate	-100	IN/s	Project
Maximum active current ramp rate	1	IN/s	Project
Maximum reactive current ramp rate	100	IN/s	Project

Table 3.3: P control mode parameters

Name	Value	Unit	Category
Time constant in power order lag	0.01	s	Type
Voltage measurement filter time constant	0.01	s	Type
Time constant in aerodynamic power response	0.05	s	Type
Maximum wind turbine power ramp rate	0.1	PN/s	Project

thesis. Among the P control mode parameters, listed in the table 3.3, only the turbine power ramp rate will be modified in order to comply with the grid codes requirements and to optimize the turbine recovery performance after faults.

The current limiter model parameters are summed up in the table 3.5, with additional look-up tables, where the maximum values of i_d and i_q can be set for the following values of the WT voltage: 0; 1; 2 p.u.

Table 3.4: Q control mode parameters

Name	Value	Unit	Category
Reactive power PI controller integration gain	5	$U_n/PN/s$	Type
Q modes 0=u; 1=q; 2=qol; 3=pf; 4=olpf	0	-	Project
Voltage PI controller integration gain	25	$I_b/U_n/s$	Type
Reactive power PI controller proportional gain	1	U_n/PN	Type
Voltage PI controller proportional gain	1	I_b/U_n	Type
User defined bias in voltage reference	1	U_n	Case
Time constant in reactive power order lag	0.1	s	Type
Power measurement filter time constant	0.01	s	Type
Resistive component of voltage drop impedance	0	Z_b	Project
Inductive component of voltage drop impedance	0	Z_b	Project
Voltage threshold for LVRT detection in q control	0.9	U_n	Type
Length of time period where post fault reactive power is injected	0.1	s	Project
Voltage dead band lower limit	0.9	U_n	Type
Voltage dead band upper limit	1.1	U_n	Type
Power measurement filter time constant	0.01	s	Type
Post fault reactive current injection	0	I_b	Project
Voltage scaling factor for LVRT current	2	I_b/U_n	Project
LVRT Q modes [0/1/2]	1	-	Project
Minimum voltage in voltage PI controller integral term	0.01	U_n	Type
Minimum reactive current injection	-1	I_b	Type
Maximum voltage in voltage PI controller integral term	1.1	U_n	Type
Maximum reactive current injection	1	I_b	Type
Maximum reactive current injection during dip	1	I_b	Type
Voltage measurement filter time constant	0.01	s	Type

Table 3.5: Current limiter model

Name	Value	Unit	Category
Maximum continuous current at the WT terminals	1.1	I_b	Type
Maximum current during voltage dip at the WT terminals	1.2	I_b	Project
Stator current limitation (0: total current, 1:stator current)	1	-	Type
Prioritisation of q control during UVRT (0: active power; 1: reactive power)	1	-	Project
Voltage measurement filter time constant	0.01	s	Type
WT voltage in the operation point where iq=0 can be delivered	-2	U_b	Type

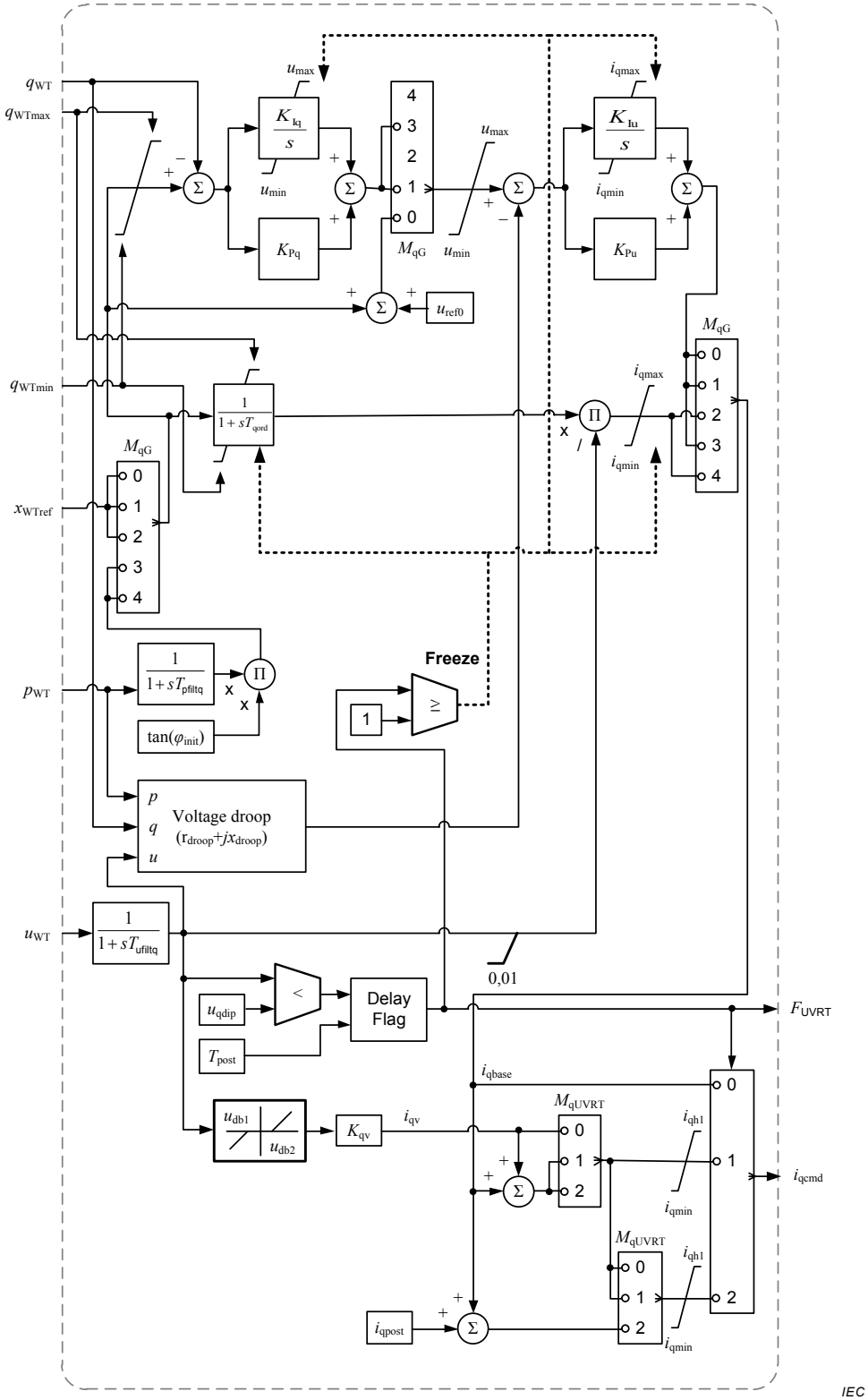

Figure 3.6: Block diagram for Q control model [18]

3.4 Grid Codes Compliance

The standard contains a large amount of parameters, which have to be set in order to model the desired wind turbine. Some of those parameters are the essential parameters, which are regulated by the grid codes. Therefore, the latest ENSTO-E grid codes have been studied in order to determine the demands, which the wind park has to comply with in order to set the necessary limitations in the control frame, representing the standard models.

The power system stability criteria have been defined previously, which are the normal design conditions for power systems, however, beyond the necessity to satisfy power system stability criteria, the designed system has to comply with the requirements of the grid codes. The grid codes requirements vary per country, however ENSTO-E network code is the grid code which is valid European-wide. It is known that in Europe, which has long history of wind energy development and typically has high wind power penetration, the latest grid codes appear to set higher demands to the wind farms. Now they have to comply with Low Voltage Ride-Through requirements, provide reactive power support to the grid, contribute to frequency and voltage control i.e., behave like a conventional power plant [21]. One of the recent challenges, introduced to the WPPs is that the newest European grid codes do not make any exceptions for the WPPs any more, the latest ENSTO-E requirements for grid connection are applicable to all generators. The requirements being harder to fulfill with weak grid connection. Due to all above mentioned, throughout the thesis work, particular attention has been payed in order to verify the grid codes compliance of the designed system.

According to the latest ENSTO-E grid codes, all list of the requirements are applicable to all generators, no exceptions are made for wind parks - they fall under the Power Park Module (PPM), as they are connected to the Network non-synchronously or through power electronics and have a single Connection Point to transmission, distribution or closed distribution network [29].

The modeled wind park is of a type D i.e. its Connection Point is at a voltage above 110 kV and its maximum capacity is above the set thresholds for all the synchronous areas [29]. The resulting requirements include certain demands, applicable for types A, B and C; as well as additional ones, which are specific for higher voltage connected generation as they have large impact on entire system control and operation. And they are to ensure stable operation of the interconnected network, allowing the use of ancillary services from generation Europe wide [29]. As far as the further requirements vary depending on the applicable synchronous area, the Nordic SA has been selected for the refine modeling parameters, its admissible voltage range is shown in table 3.6. All the demands in the grid codes are stated with respect to the PCC.

Table 3.6: Admissible time periods and voltage range for the Nordic Synchronous Area

Time period	Voltage range, p.u.
Unlimited	0.9 - 1.05
60 minutes	1.05 - 1.10

One of the key requirements, limited by the Low Voltage Ride Through curve for the type D Power Park is shown on the figure 3.7. t_0 is the time, when the fault occurs, t_{clear} is 0.14-0.25 seconds after the fault; t_{rec} is 1.5-3 seconds. Furthermore, during the period of faults reactive current injection is demanded from the PPM up to 1 p.u. of the short term dynamic current rating [29], while nothing is mentioned regarding the active current.

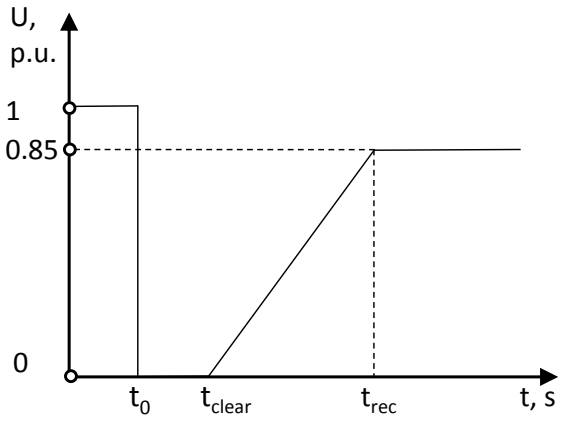

Figure 3.7: LVRT curve for the PPM type D

It must be noted, that the grid codes do not specify the following conditions, which are of a great importance in terms of this work [29]:

- The minimal SCR to which the grid codes are applicable
- LVRT conditions for the calculation of the pre-fault minimum short circuit capacity at the Connection Point
- Conditions for pre-fault active and Reactive Power operating point of the Power Generating Module at the Connection Point and Voltage at the Connection Point
- Conditions for the calculation of the post-fault minimum short circuit capacity at the Connection Point

The above-mentioned parameters are to be set by each transmission system operator (TSO) individually, as well as the protection schemes and settings.

For the maximum active power output, the steady-state $U - Q/P_{max}$-profile shall not exceed the envelope, represented in figure 3.8 and the position of the envelope within the limits of the fixed outer envelope in figure 3.8. For the Nordic synchronous area the maximum range of Q/P_{max} is 0.95 and maximum range of steady state voltage is 0.15. The exact position of the inner envelope is supposed to be defined by the TSO. Therefore, the exact values of the WPP reactive power capabilities will be varied throughout the work, in order to achieve the best performance. These limitations are implemented in the look-up table within the current limitation model in the control frame, depicted on figure 3.5. The initial limits of the Q range have been set to ± 0.4 p.u.

The reactive power output of the WPP at the PCC must be zero, when the voltage at the PCC equals to its setpoint. In case of disturbance the WPP must achieve 90% change in Q output within a range of 1 - 5 seconds (defined by TSO) and settle to the $Q_{max} \pm 5\%$ within 5 - 60 seconds(defined by TSO). That requirement is fulfilled by setting the limits of the maximum reactive current ramp rate in the generator control frame, shown on figure 3.4.

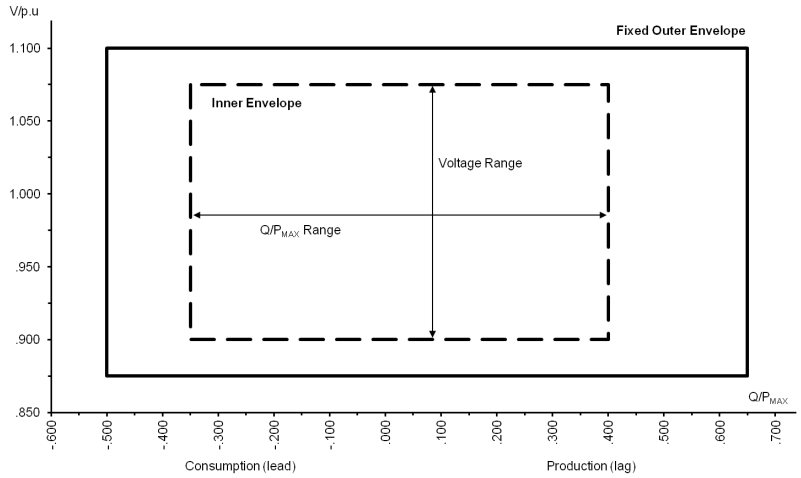

Figure 3.8: $U - Q/P_{max}$ profile of a Power Park Module at the Connection Point, expressed by the ratio of its actual value and its nominal value in per unit, against the ratio of the Reactive Power (Q) and the Maximum Capacity (P_{max}). [29]

The reactive power control requirement states, that the Power Park Module shall be capable of providing Reactive Power automatically by either Voltage Control mode, Reactive Power Control mode or Power Factor Control mode [29], that corresponds to the three Q control modes implemented in the used WT models.

4 | Simulations

This chapter contains the entire work process, which lead to the thesis objectives achievement and result in the main conclusion of the thesis. First, the system has been loaded with two different sets of parameters, representing strong and weak grids, analyzing the fundamental differences of the performances. The obtained results and derivations prove the necessity of the shunt capacitances inclusion into the model, which has been carried out with the following repetition of the simulations. Section 4.3 includes the small-signal stability analysis of the modified system and the subsequent controllers improvement in order to achieve stable operation. The last section 4.4 includes the transient analysis of the system, namely investigation of its response short circuit fault, with the further system optimization.

4.1 Simulated Cases

Two generic sets of parameters have been used in order to represent, correspondingly, strong and weak grid models, described in table 4.1 in terms of their Thevenin impedances and SCRs seen from the PCC.

Table 4.1: Investigated case parameters

	Strong Grid	Weak Grid
Z_{th}, p.u.	0.02+i0.2	0.1+i1
SCR_{PCC}	5	1

For each case the following reactive power control modes have been investigated:

- Voltage control, $U_{ref} = 1$p.u.
- Reactive power control, $Q_{ref} = 0$
- Power Factor control, $PF_{ref} = 0.9$

The open loop reactive power control and open loop power factor control modes are not considered, as they are only applicable in couple with the closed-loop plant-level control [18]. The selected control conditions are based on the possible objective functions:

- Voltage control with 1 p.u. setpoint due to the necessity to keep the PCC voltage within the narrow limits, dictated by the grid codes.
- Zero reactive power is the desired goal due to the fact, that it gives possibilities for the converter size reduction, thus the total costs reduction. The objective is being intensively researched, for example in [30].

- Even though the modern WPPs aim to operate at unity power factor [31], PF control mode has 0.9 setpoint due to the fact, that setpoint of 1 would duplicate the performance of zero Q setpoint, because the two modes use the same reference value (Q_{WT}). 0.9 PF was selected as a minimum realistic value for the modern WTs [32], taking into account the Q support requirements by the grid codes.

An integral part of the correct controllers behavior is the correct initialization. Therefore, all the case parameter must be updated prior to initialization [18], both WT parameters and grid parameters. The models are initialized by the load flow, i.e. it sets the initial values of the currents and voltages, as well as controllers reference values. For the Power Factor control mode, unlike the voltage and reactive power control, the reference setpoint cannot be changed throughout the simulation. It is necessary to fulfill certain restrictions in order to be able to carry out initialization after the convergent load flow: the voltage at the WT terminal must be higher, than the UVRT threshold from the table 3.4. The parameters, obtained after load flow calculation must correspond to the target values of the reference parameters

Active power ramp from 0.01 p.u. (the minimum active power supplied at cut-in wind speed [33]) to 1 p.u. have been carried out within a time span of 10 seconds. It must be noted, that the applied power ramp does not represent the wind speed variations, but a sequence of subsequent load flow solutions, due to the requirements of the IEC models and the nature of the RMS simulations tool.

The integration time constant has been fixed at 0.005 s., as dictated by the IEC standard, which states, that the models have not been validated for other time steps [18]. Therefore all the time constant in the simulation model must not exceed 0.01 s, i.e. double of the integration time constant [18].

The following parameters of interest have been recorded throughout the power ramped:

- Active power of the WT
- Reactive power of the WT
- Voltage magnitude at the PCC
- Voltage angle δ at the WT bus
- dq-currents of the WT converter

The results have been processed and further dependences have been plotted with Matlab.

4.1.1 PV and PQ Curves

In order to demonstrate the achievable maximum power transfer, the traditional PV curves representation is used, as the relationship between P and V is essential [24]. It must be noted, that on the following curves P is the active power, supplied by the WT and U is the voltage at the PCC.

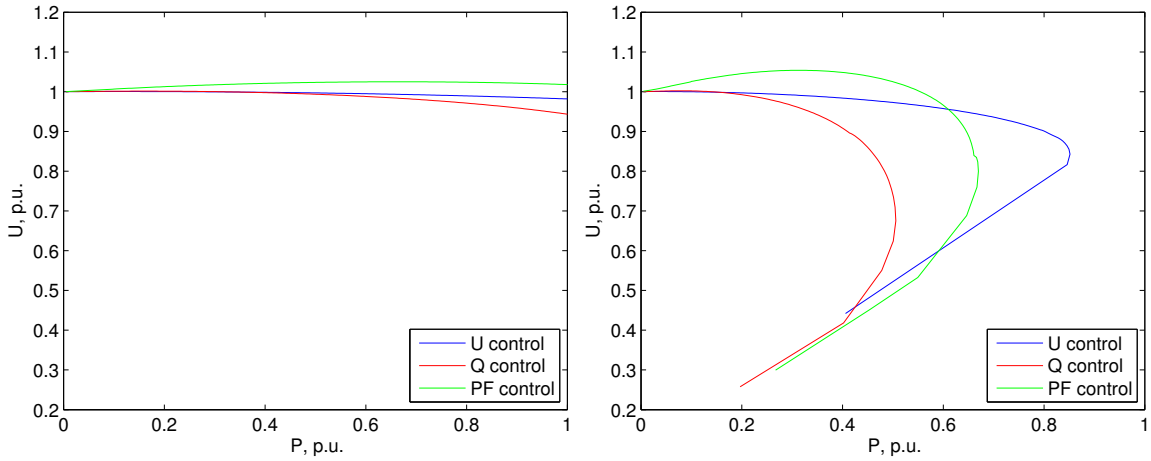

(a) (b)

Figure 4.1: PV-curves for strong (a) and weak (b) grids

The obtained curves demonstrate the considerable influence of the grid strength on maximum transferable active power. The strong grid operation is stable throughout the simulation and the maximum transferable active power is much higher, then 1 p.u. therefore the tip of its nose curve lies beyond the limits of the applied power ramp. On the contrary, for the weak grid condition the PV curve demonstrate smaller active power transfer capabilities, and for all the control modes critical operating point occurs at $P < 1$ p.u. and the voltage instability is obvious.

The first general observations clearly point out that the U control mode performs considerably better, compared to the Q control and PF control modes. The curve flatness resembles the curves, which take place on condition of the strong grid. Poor performance of the Q control is determined by the zero reactive power setpoint - low reactive power support results in low voltage support, therefore voltage continues to drop in couple with active power supply increase. When the Q setpoint is 0.1 p.u. the Pmax slightly increases to 0.55 p.u., but the steady state voltage at lower power outputs increases considerably, further Qref increase results in its unacceptably high value. The performance of the PF control mode is also not flexible: a low P output the voltage becomes too high (due to the reactive power injection, which is higher, than necessary), while for higher power outputs the reactive power support becomes insufficient, resulting in voltage decrease.

Pmax depends on voltage, and voltage, in its turn, depends on reactive power supply, In order to explain the observed phenomena, an insight into reactive power injection must be taken. Figure 4.2 demonstrates another conventional PQ curve, known as Power Circle Diagram, which can be also interpreted as the trajectory of the sending end voltage with the receiving end voltage vector pointing the coordinates origin with both vectors originating in the center of the circle [10]. It is known, that the maximum active power occurs, when the tangent to the curve becomes vertical [10]. On the figure for weak grid the maximum active power is reached and is marked with o, while for the strong grid the maximum active power is beyond the ramp limit. The strong grid response is far from the classical circumference due to the following reasons:

- For the Q control mode the reactive power value is kept equal to zero, therefore the curve is horizontal and coincides with y-axis as long as the control is taking actions
- When PF is kept constant at the PF control mode, the curve is a straight line, which is tilted with angle ϕ
- For the U control mode the curve actually resembles the circle segment of a large radius

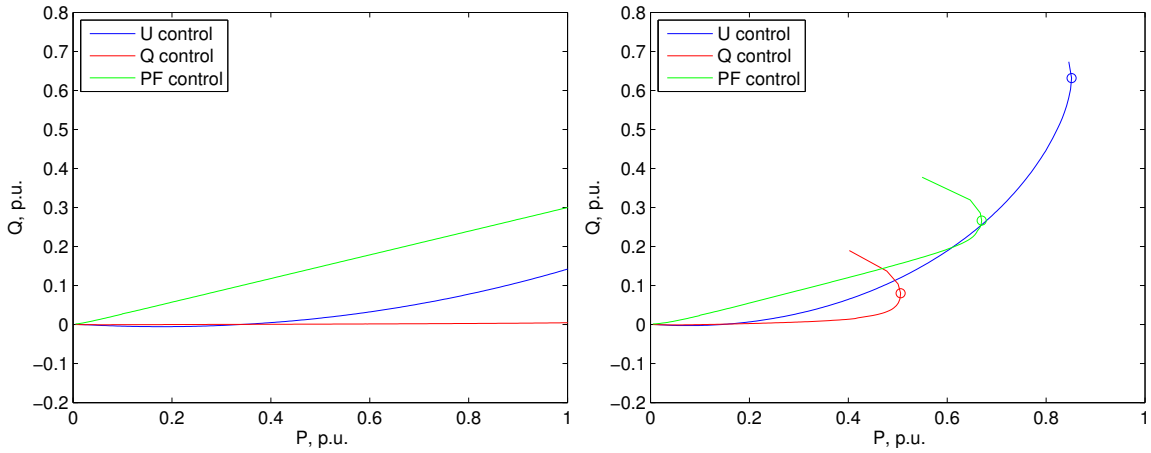

(a) (b)

Figure 4.2: PQ-curves for strong (a) and weak (b) grids

Analysis of the curves for weak grid explain the reason for the U control mode better performance: high reactive power injection supports the voltage at the admissible level, while for Q control and PF control the Q injection is limited. In this case the turbine is supplying 0.6 p.u. reactive power to the grid, while the active power output is 0.85, that is still within the turbine capability, but the value is quite high in terms of feasibility. In case of the Q control the control conditions are violated when the P reaches 0.4 p.u. - the turbine start supplying reactive power to the grid, in spite of the zero setpoint. The same happens PF control modes - up to 0.6 p.u. active power the curve resembles the one, observable at strong grid, i.e. $\tan\phi$, after this point the control conditions are not fulfilled any more and the curve changes its shape. The reason of the control conditions violation can either be low proportional gain of the voltage controller, or the fact, that the reactive power support, delivered when those control modes are on are insufficient to maintain the voltage within its desired limits. The high amount of reactive power, demanded from the turbine can partially be explained by the absence of capacitances in the system - the turbine has to cover all the reactive power demand along the transmission line, the issue is going to be explained int eh next section.

4.1.2 P-δ Curves

Another dependence of interest is power-angle relationship. In this case angle δ is the voltage angle at the WT bus, as the grid bus is the slack bus and, therefore, its voltage angle is zero.

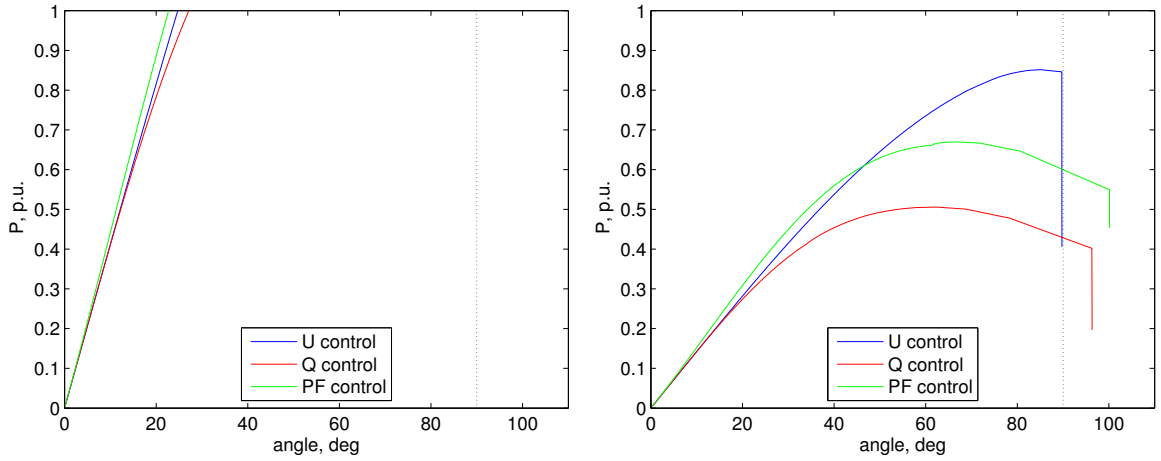

Figure 4.3: Pδ-curves for strong (a) and weak (b) grids

Analogically, in the case of strong grid, the angle change along the power ramp is much smaller, than in the case of weak grid. For the weak grid voltage control mode the voltage collapse occurs, when voltage angle approaches 90°. From the power system fundamental principles it is known, that for the two-machine system this value corresponds to the maximum steady state power, that can be transmitted between the two machines. However the maximum magnitude of the active power, obtained throughout the simulation does not exceed 0.85 p.u. In order to investigate the nature of the phenomena, it is necessary to refer to the fundamental formula of the active power transfer in the two-machine system:

$$P = \frac{E_S \cdot E_R}{X_T} \cdot \sin\delta \tag{4.1}$$

Where E_S and E_R are the voltage magnitudes at the sending and receiving ends correspondingly, X_T is the line inductance between the sending and receiving ends, and δ is the angular separation between the ends.

For the investigated case the E_R value is fixed at 1 p.u., because the sending end is the slack bus. E_S is the WTG terminal voltage, and its value must be in range of [0.9 1.1] p.u. due to relay protection setting as it is normally stated in general specification [34]. X_T is a constant value:

$$X_T = X_{int} + X_{th} \tag{4.2}$$

Where X_{int} is the inductive component of the impedance between the WT and the PCC, namely reactance of the WT transformer, internal cable and the WP transformer. X_{th} is the inductive component of the Thevenin impedance between the PCC and the Grid.

$$X_T = 0.25 + 1 = 1.25 p.u. \tag{4.3}$$

From the formula 4.1, separation angle can be expressed as:

$$\delta = \arcsin \frac{P \cdot X_T}{E_S \cdot E_R} \tag{4.4}$$

Substituting the known values,

$$\delta = \arcsin \frac{P \cdot 1.25}{[0.9 \div 1.1] \cdot 1} \tag{4.5}$$

Therefore, due to the presence of sinus, the possible solutions are constrained by:

$$\left| \frac{P \cdot 1.25}{[0.9 \div 1.1]} \right| \leq 1 \tag{4.6}$$

Therefore, the maximum transferable power for the given system is:

$$P_{max} = 0.88 p.u. \tag{4.7}$$

on condition of the WT terminal voltage is at its maximum limit. This is the maximum transferable active power for the studied simplifies system, with negligible resistances and capacitances.

Therefore, the capabilities of the simplified conventional power system modeling, i.e. wen transmission line is represented by the inductive reactance only [24] can be derived for the low SCR studies. In order to connect 1 p.u. of active power to the system, represented by two-machine system, connected by the transmission line with negligible resistance and capacitances, the following SCR limits have been derived, based on formula 4.1 and constraints 4.6.

$$\left| \frac{P \cdot X_T}{E_S \cdot E_R} \right| \leq 1 \tag{4.8}$$

Taking into account, that in per unit $SCR = Z_{th}^{-1}$, the formula 4.2 becomes as follows:

$$X_T = X_{int} + \frac{1}{SCR} \tag{4.9}$$

After substituting into 4.8, assuming P=1 p.u., because WPP rated power equals to the system base power [18]; $E_R = 1$ p.u., because grid is modeled as a slack bus, the final constraints become:

$$X_{WT} + \frac{1}{SCR} \leq E_S \tag{4.10}$$

After simplification, sticking to the maximum limits of the constraints:

$$SCR_{min} = \frac{1}{E_{S_{max}} - X_{int}} \tag{4.11}$$

$E_{S_{max}}$ being the maximum voltage at the WT converter terminals, which is normally assumed to be 1.1 p.u., but might vary depending on the manufacturer specification. $Xint$ is the corresponding reactance between the WT bus and the PCC. The resulting SCR_{min} is the absolute minimum for the system with negligible resistances. In case of the system modeling with considerable resistance ($R \neq 0$), like in the simulated case, this value represents the maximum power at the sending end (WT bus in this case). The effect of the resistance is the presence of losses and the consequent difference between the sending and the receiving end maximum active power [10].

For the modeled WPP, the corresponding value is:

$$SCR_{min} = \frac{1}{1 - 0.25} = 1.18 \tag{4.12}$$

That gives the explanation of the occurring blackout, as the modeled system has a SCR of 1, which is lower, that admissible level. Therefore it can be concluded, that the derived formula 4.11 sets the minimum SCR for the simplified modeling, containing only inductive components of the impedances. In cases, when studies for the systems with lower SCR are needed, it is crucial that the capacitances are included in the studied system.

4.2 Modified System

The majority of the research papers, carried out on the topic of low SCR connection use simplified line modeling, represented as series inductance, as in the papers [3], [4], [8], [5], [7], [6], [35], [36], [37], [38], while only few include shunt capacitances, for example papers [34] and [39]. Therefore, taking into account the above-derived equations, the results of the simulations, where shunt capacitances are neglected possess higher SCR limitation, especially in terms of the transmission capacity.

Due to the above-mentioned findings, certain changes have been implemented into the PowerFactory model of the system. A cable connection has been introduced between the PCC and grid impedances. The cable replaces the 0.05 p.u. inductive reactance, which has previously been included into Z_{th}.

4.2.1 Cable parameters

The cable does not represent parameters of any specific manufacturer, for the generalization purposes, as the actual parameters can vary greatly, based on the design priorities. Nevertheless, certain limitations apply. Primary, the cable has to comply with the current-carrying capabilities, which are calculated as:

$$I_{1\phi min} = \frac{\frac{S_{3\phi}}{U_{3\phi}}}{\sqrt{3}} \tag{4.13}$$

where $I_{1\phi min}$ is the minimum steady-state current-carrying capacity of the cable per phase, $U_{3\phi}$ is the line-to-line voltage of the transmission line and $S_{3\phi}$ is the maximum transmitted apparent power, which can be calculated as:

$$S_{3\phi} = \sqrt{{P_{3\phi}}^2 + {Q_{3\phi}}^2} = \sqrt{(100 \cdot 10^6)^2 + (60 \cdot 10^6)^2} \approx 120MVA \tag{4.14}$$

Substituting into 4.13:

$$I_{1\phi min} = \frac{\frac{120 \cdot 10^6}{132 \cdot 10^3}}{\sqrt{3}} \approx 525A \tag{4.15}$$

Therefore, only the cables with current-carrying capacity above this value are considered.

Table 4.2: Parameters of the various 132kV cables [40]

Type	I_{max}, A/ϕ	R, Ω/km	X, Ω/km	B, μS/km
132 kV land cable, Cu, flat	535	0.062	0.116	97
132 kV land cable, Al, flat	764	0.026	0.177	78.5
132 kV sea cable, Cu	835	0.105	0.129	66

As can be seen from the table 4.2, different cables have considerable variations in the key parameters, therefore the modeled cable results in Z=0.05 p.u. can represent, for instance 50 km of aluminum cable or 60 km of copper cable, both of the cases being realistic from the WPP connection point of view and both being considered as relatively long connection lines [3].

Therefore, the modeled cable has the following parameters:

Table 4.3: Parameters of the modeled cable

Type	I_{max}, A/ϕ	R, Ω/km	X, Ω/km	C, μF/km	l, km
132 kV land cable, Al	600	0.02	0.2	0.25	50

That results in 0.05 p.u. reactance and 0.005 p.u. resistance, total shunt susceptance being 3436 μS, resulting in reactive power injection:

$$Q_C = \frac{U^2 \cdot B}{S_{base}} = \frac{123 \cdot {10^3}^2 \cdot 3436 \cdot 10^{-6}}{100 \cdot 10^6} \approx 0.6p.u. \tag{4.16}$$

The cable is modeled through the PowerFactory line element (ElmLne), which represent the underground cable parameters by setting the type to cable (TypCab). Due to large amount of injected reactive power and the cable length it was decided to use the line model as a distributed parameter instead of the conventional lumped parameter (π - equivalent) [27].

4.2.2 Reactive Power Compensation

Known issue for the cable connection is the reactive power balance, therefore, in order to confirm, that the cable is injecting the reactive power it is necessary to determine its SIL according to the previously introduced formula 2.6.

$$P_{SIL} = \frac{132 \cdot 10^{3^2} / \sqrt{\frac{4 \cdot 10^{-3}}{0.25 \cdot 10^{-6}}}}{100 \cdot 10^6} = 1.38 p.u. \tag{4.17}$$

This value exceeds the transferred power, therefore, the cable is producing considerable amount of reactive power in normal operation mode. Therefore, compensation is needed. According to [41], the necessary reactive power compensation for 50 km of the 132kV cable is 32.5 MVar at both sides. However in [41] it was determined, that the compensation on both sides has only considerable effect in case of necessity to transfer larger amount of active power along larger distances, as depicted in figure 4.4.

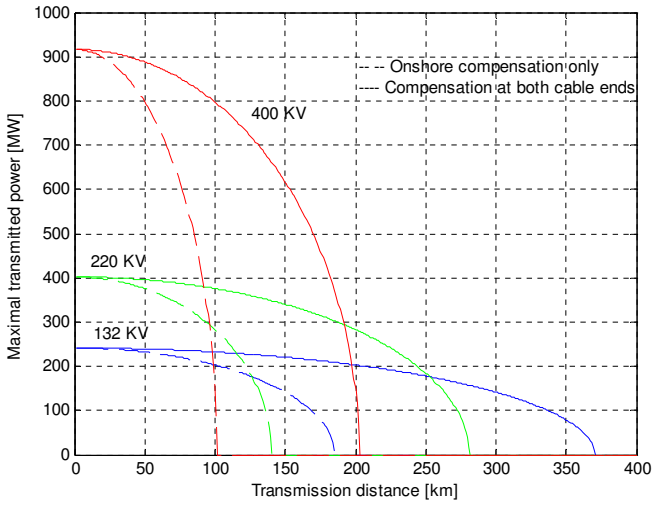

Figure 4.4: Limits of cables transmission capacity for different voltage levels, both compensation solutions [42]

Therefore, based on the conditions of minimum necessary compensation it was decided to use one-side/onshore compensation only. Therefore the designed system is equipped with additional element - shunt reactor (ElmShnt) with the following controller parameters:

- 10 steps of 6 MVars
- switchable
- remote control enabled with the reference to the PCC bus
- 0.1 s controller time constant
- 0.05 p.u. dq/dv sensitivity.

However it has been noted throughout the simulations, that along the power ramp from 0.1 p.u. a phenomena of certain interest occurred: with increase of active power output the reactor control switch steps down and when the active power of the WT reaches its rated value, the step is set to zero, as shown on figure 4.5

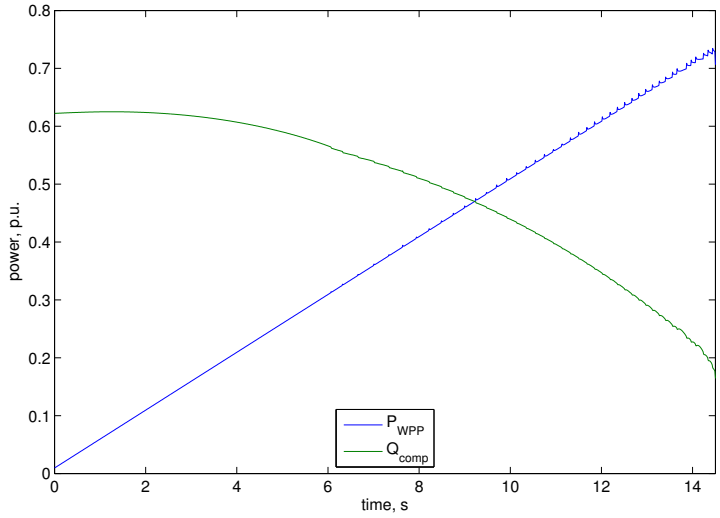

Figure 4.5: Change of reactive power compensation along the active power ramp

The reason behind the reactor controller behavior is that with increase of active power output the voltage at the PCC is becoming lower, therefore reducing the need of compensation, when the active power of the WT reaches its rated value the necessity of compensation is eliminated.

The fact that the compensation is not needed lies in the Weak Grid condition itself: due to large grid inductance, the grid impedance is constantly absorbing large amount of reactive power, therefore, the reactive power, produced by the cable is immediately absorbed by the grid.

That allows to conclude, that in cases, when the connection cable is used between a WPP and a weak grid, there is no need for reactive power compensation at high active power output. There is, nevertheless, the need to keep the reactive power flow direction constant, namely from the wind turbine into the grid. That can be achieved by keeping the voltage at the Offshore Bus lower, that at the PCC. Which, in its turn, can be achieved by controlling the WT reactive power injection.

Taking into account all above-mentioned the decision has been taken not to include any reactive power compensation, but to compensate the reactive power, injected by the cable by means of WT converter. The decision requires the turbines to be grid-connected at all times [43], but it does not require increase of the converter size due to the fact, that high reactive power absorption is required only at low reactive power outputs and vice versa, as seen on the figure 4.5. Apparent power determines the converter size, it has been set to 1.2 p.u., as calculated by the formula 4.14, when the turbine converter is used for the reactive power compensation the apparent power for the low and high active power outputs are 0.67 p.u. and 0.77 p.u. correspondingly.

4.2.3 Simulation Results

First of all it must be noted, that all the further studies will be carried out for the voltage control mode of the reactive power controller for the weak grid, as it, without any doubt is performing the best results, comparing to the Q control and PF control modes due to the following reasons:

- The maximum transmittable reactive power is much higher for this mode. It can be explained by the fact, that the the Q control and PF control limit the Q, which is necessary in order to increase the voltage, while the U control doesn't limit the reactive power, therefore it is always sufficient to maintain the voltage at the admissible level. As far as the value of the transferable active power depends on voltage, the higher amount of active power in case of U control mode is understandable.
- The U control mode is always aiming to keep the voltage at 1 p.u., therefore for the fault calculations, for example, the pre-fault conditions calculation will be more predictable, while for the PF control or Q control the voltage might be sticked to higher or lower limits correspondingly. Additional effort must be made in order to prevent the voltage of entering the LVRT mode, as that would result in undesirable voltage step and oscillations.
- The voltage control mode has only one PI control loop, unlike the remaining ones (depicted on at the top of figure 3.6). That eases the controller tuning, because in the voltage control the tuning is more straightforward.

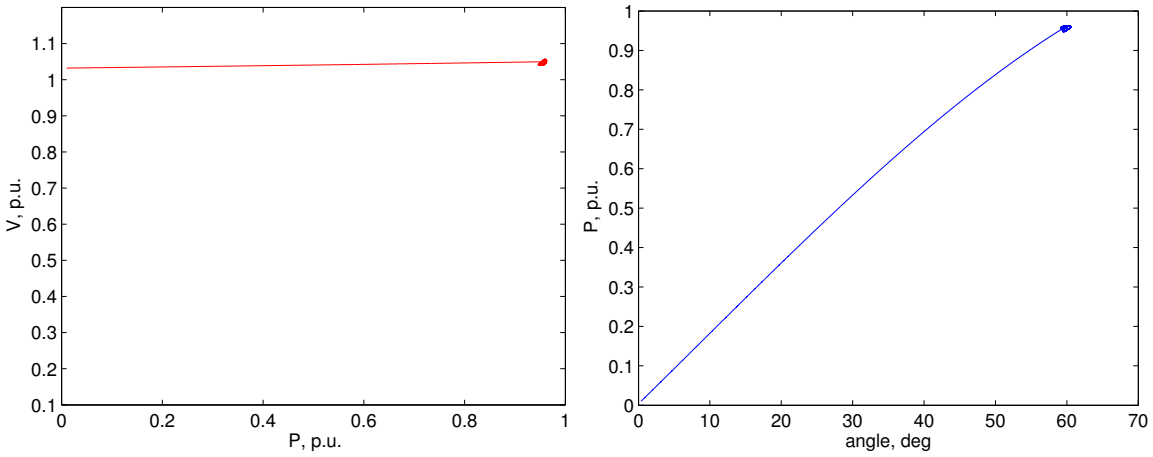

(a) (b)

Figure 4.6: PV (a) and P-δ curves (b) for the modified grid model

The same power ramp have been applied to the modified grid and considerable improvement of the simulation results has been observed. Both PV (figure 4.6 a) and P-δ (figure 4.6 b) curves demonstrate higher flatness, compared to the analogous curves on figures 4.1 b and 4.3 b correspondingly. However the total power does not reach the commanded reference of 1 p.u. and oscillations can be observed at maximum power point. That behavior of the system is defined as oscillatory instability, which is one of the small signal stability problems. It is being often faced during the modeling of a power

system with low SCR and high amount of power electronic devices. The instability might be caused by insufficiently accurate controller settings, corresponding to one of the control mode [24]. In order to verify the essence of the instability, small signal stability analysis has to be carried out.

4.3 Small-Signal Stability

In order to determine the reason of the occurring oscillations, the small-signal stability analysis has to be carried out. The eigenvalue analysis is known to be the most powerful tool for the oscillatory stability studies [44]. The Modal Analysis tool in DIgSILENT PowerFactory is using the numerical methods for iterative calculation of the eigenvalues. The classical QR/QZ method has been selected, as it supports the PWM converter model [44], which is used in type 4 WT.

The eigenvalue analysis has been carried out for the operating point of the highest active power injection, for which the load flow solution still converges, which is $P_{WT} = 1$ p.u., $Q_{WT} = 0.25$ p.u.

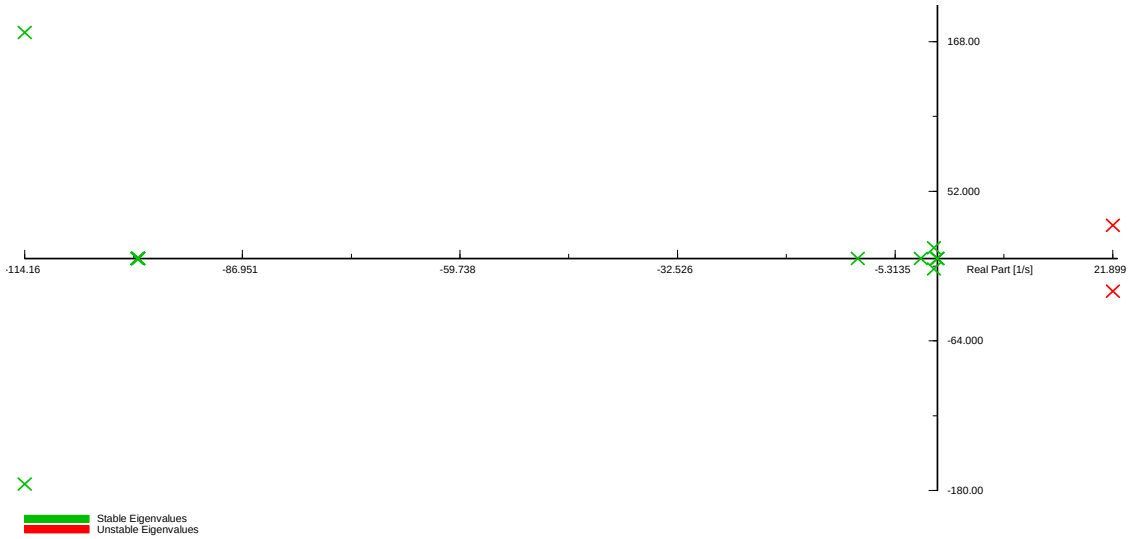

Figure 4.7: Eigenvalue plot for the operating point P=1 p.u., Q=0.25 p.u.; controller gains Ki=25, Kp=1.

According to Lyapunov's first method, when at least one of the eigenvalues has a positive real part, the system is unstable [24]. Two unstable poles can be observed on the eigenvalue plot, therefore, the system is considered to be unstable. The location of the poles indicate oscillatory instability, as the poles are complex conjugated and have positive real part. State variable with the highest participation factor is the voltage angle δ. The coordinates of the observed mode are: Real part=21.899 1/s Imaginary part = 24.999 rad/s. It is known, that the real component of the eigenvalues gives the damping and the imaginary component gives the frequency of oscillations; a negative real part represents a damped oscillation while a positive real part represents oscillations of increasing amplitude [24]. Therefore, complex pairs of eigenvalues are expressed as:

$$\lambda = \sigma \pm j\omega = 21.899 \pm 24.999 \tag{4.18}$$

The values of σ and ω are used for the analysis of the oscillations. Oscillatory frequency is calculated as:

$$f = \frac{\omega}{2\pi} = \frac{24.999}{2\pi} = 3.979Hz \tag{4.19}$$

Period:

$$\nu = \frac{1}{f} = \frac{1}{3.979} = 0.251s \tag{4.20}$$

The damping ratio is calculated as:

$$\psi = \frac{-\sigma}{\sqrt{\sigma^2 + \omega^2}} = \frac{-21.899}{\sqrt{21.899^2 + 24.999^2}} = -0.725 \tag{4.21}$$

Time constant of the decay amplitude :

$$K = \frac{1}{|\sigma|} = \frac{1}{|24.999|} = 0.001 \tag{4.22}$$

Table 4.4: Oscillation Parameters of the unstable poles

Name	Value	Unit
Frequency	3.979	Hz
Period	0.251	s
Damping	-21.899	1/s
Damping ratio	-0.725	-
Damping time constant	0.038	s
Ratio of amplitudes	0.001	-

The parameters of the oscillations are summed up in table 4.4. The frequency range of interest, which affect stability is 0.1...10 Hz [45], the observed mode falls within this limit; frequency around 4Hz speaks for a control (local) mode. The damping ratio is a negative value, which speaks for the divergent oscillations.

The influence of the SCR value on the network dominant eigenvalues for the systems with fully-rated converter wind turbines have been previously studied in academia [46]. Therefore, the further studies are concentrated on the effect of the controller influence. The analysis confirms the instability of the controller, which is understandable, as controllers are originally tuned for the strong grid [4], i.e. having SCR higher, than 3, while in the weak grids the dV/dQ sensitivity is significantly higher, i.e. same reactive power variations will cause much higher voltage fluctuations in the weak grid. Therefore, parameters of the voltage controllers are crucial.

In order to investigate the processes, occurring in the WT converter, the insight into the converter dq-currents has been taken, as depicted on figure 4.8. The dq-currents of the converter in couple with their references have been plotted for the strong and weak grids models, used in the analysis in the

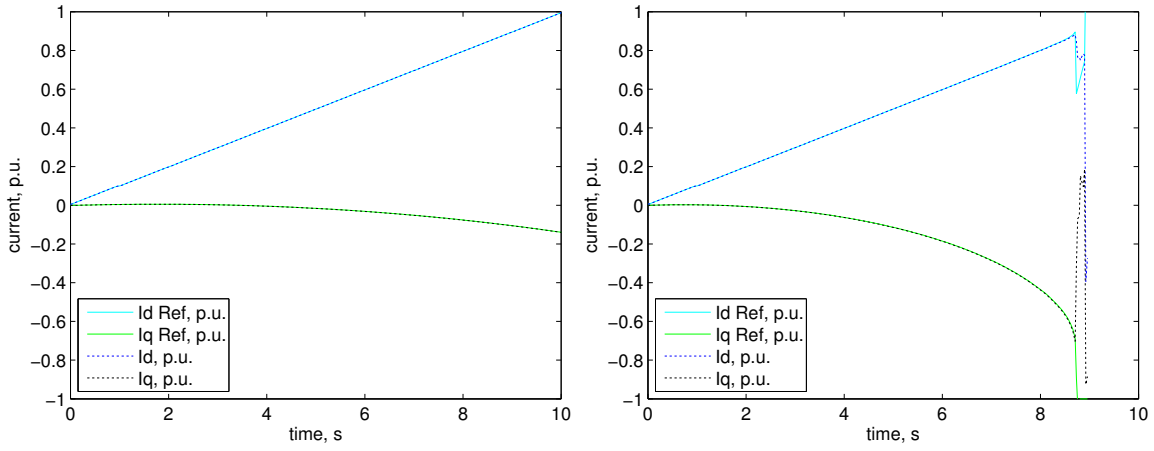

(a) (b)

Figure 4.8: dq currents and their references for strong (a) and weak (b) grids

previous section. The only parameters of a difference for the two cases is the magnitude of the grid impedance. It must be noted, that the sign convention, used in PowerFactory has certain peculiarities: the direction of the current from the converter into the grid for d-current has positive value, while for the q-current it is negative [47]. Therefore, even though on the graph the currents of the converters have opposite values, they are both have the same direction. It can be noted, that the same values of the controller gains in the cases of strong and weak grid demonstrate drastically different performance. It can be observed from the graphs, that for the strong grid case d and q currents follow the reference precisely along the power ramp, while for the weak grid case at certain level of active power injection, the converter can not follow the current references accurately.

As it is known from the control theory basics, the variable responsible for the reference tracking is the controller proportional gain: the higher the proportional gain, the better is the reference tracking, however, it is known as well, that the exceedingly high value of the proportional gain can lead to the loss of system stability [48]. Taking into account the behavior of the converter in the weak and strong grids correspondingly, it can be concluded, that the proportional gain, which is sufficient to ensure the reference tracking in the strong grid is not sufficiently high to perform well in the weak grid, therefore it has been decided to increase the value of the voltage controller proportional gain. That decision corresponds to the previously published findings on WT control in weak grids. For example, the reference [4] suggest, that in case of instability the proportional gain of the controller must be increased to a value, higher than 1 (which is the default tuning in the PowerFactory model).

Therefore, the proportional gain has been increased stepwise in order to determine the maximum K_P value, which would still perform good stability. It was noticed, that for the studied weak grid model the increase in K_P also results in stability increase, of to the value of 4.5; further increase in K_P results in the poles moving towards the right-hand plane. Therefore it was concluded, that the proportional gain $K_P = 4.5$ gives the best stability, i.e. the poles have the highest negative real part and the damping is the highest. The corresponding small-signal stability plot is depicted on figure 4.9. The variation of the integration gain do not have significant effect on the stability. However it can be observed, that there are two complex conjugated poles in the left-hand side of the plane, which are located very close to

the coordinates origin. State variable with the highest participation factor is the voltage measurement filter time constant, and therefore integration gain will be modified in order to eliminate the dominant time constant [49]. The controller tuning peculiarities will be discussed in detail in chapter 5.

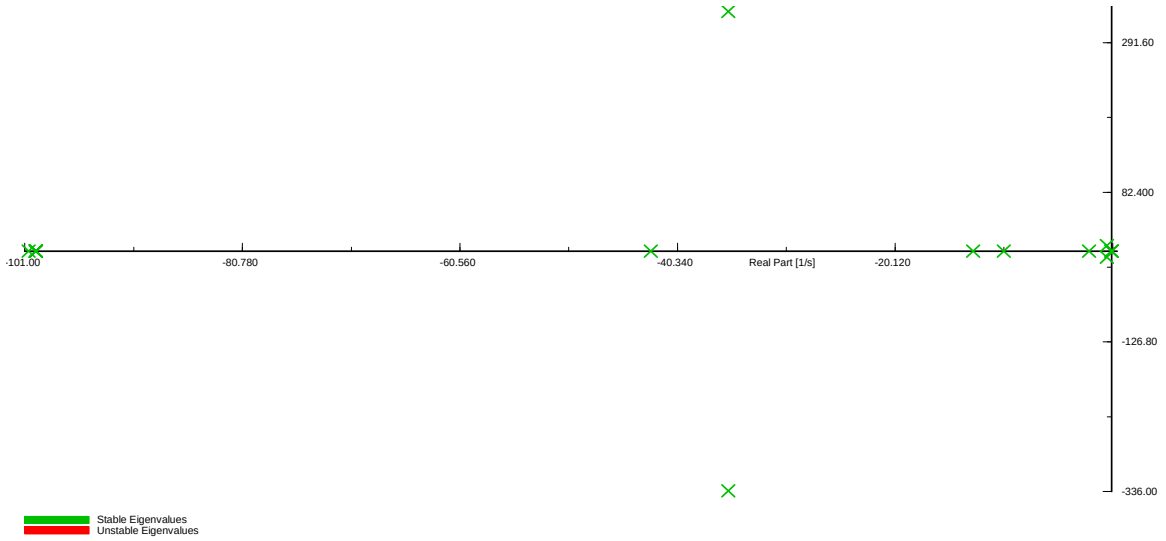

Figure 4.9: Eigenvalue plot for the modified controllers at he operating point P=1 p.u., Q=0.25 p.u.; controller gains Ki=25, Kp=4.5.

A considerable improvement of the eigenvalue plot can be observed on figure 4.9: a pair of the oscillatory poles have been eliminated and another one has moved further away from the real axis.

The coordinates of the observed mode are: Real part=-32.364 1/s Imaginary part = -334.536 rad/s The corresponding oscillation parameters have been calculated according to the formulas 4.19-4.22 and are represented in the table 4.5.

Table 4.5: Oscillation Parameters of the poles after controller adjustment

Name	Value	Unit
Frequency	53.243	Hz
Period	0.019	s
Damping	32.364	1/s
Damping ratio	0.096	-
Damping time constant	0.031	s
Ratio of amplitudes	1.836	-

According to Lyapunov's first method, when the eigenvalues have real parts zero, it is not possible to determine stability. In the system, there are three modes, having real part zero, they are all located in the coordinates origin. The corresponding state variable is the voltage angle of controllable voltage source. The value is fixed to zero, due to the nature of the block. The oscillatory poles, which are close to the axis origin represent the state variable: generator inertia in the two-mass model. This value is a type parameter and cannot be changed. Even though eigenvalue analysis is considered to be the best tool for the small-signal stability, it is necessary to verify the results with the dynamic simulations. The reason is that IEC 6400-27-1 states, that the elaborated models "have not been developed explicitly

with eigenvalue calculation (for small signal stability) in mind [18], due to the fact, that the models are considerably simplified, which might affect the linearizion for the eigenvalue calculation.

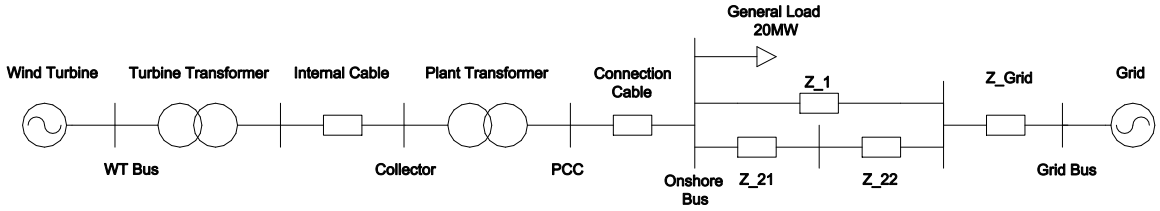

Figure 4.10: Small disturbance application - load connection

The results have been verified with the dynamic simulations, figure 4.10 demonstrates the 20 MW load has connection to the Onshore Bus, as it is the closest realistic load bus to the WT, at t=10 seconds, and the system response for the both cases are shown on figure 4.11(b). The periods of the occurring oscillations relate them to observed oscillatory modes. The figure 4.12 demonstrates the enlarged fragment of the figure 4.9 for the check of the oscillation period. It is seen, that the period of oscillations, obtained through the dynamic simulations corresponds to the period, obtained through the eigenvalue analysis. That is speaking for the sufficient accuracy of the models for the eigenvalue analysis.

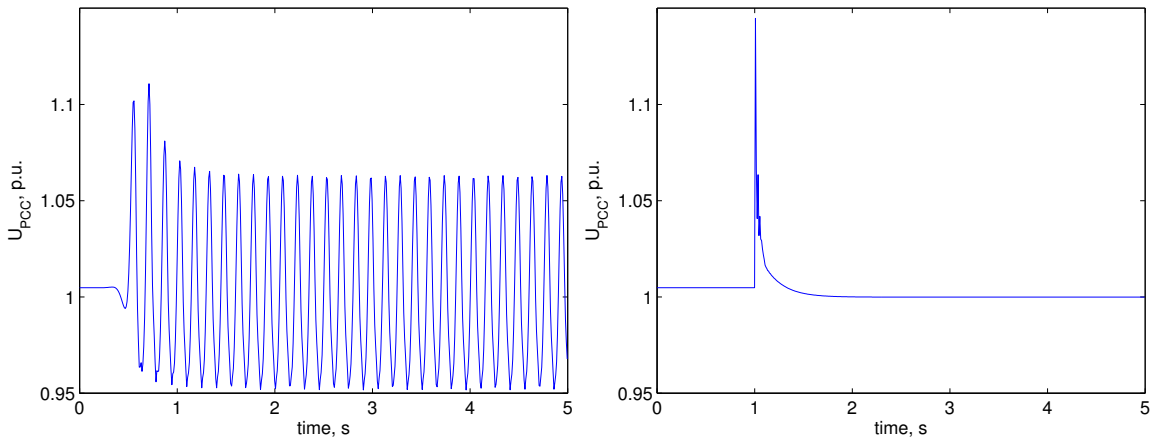

Figure 4.11: Voltage response to a small disturbance with the original (a) and the modified (b) controllers

In order to be consistent, a dynamic simulation has been carried out for the original the system as well. A remarkable phenomena has been observed: after a successful load flow solution, initialized with an operating point of P=1 p.u., Q=0.25 p.u., the dynamic simulations show occurrence of the undamped oscillations prior to applying any disturbances, as it can be seen on figure 4.7. The period of the oscillations is 0.25 seconds, which corresponds to the one, obtained via eigenvalue analysis. Therefore, eigenvalue analysis results have been approved. Additional observation has been noted, that for the weak grids studies the converging load flow solution does not always guarantee a stable steady state behavior of the simulated system. Therefore, further load flow solutions have to be verified

by a dynamic simulation of the no-event RMS solution in order to track possible instability due to controllers tuning.

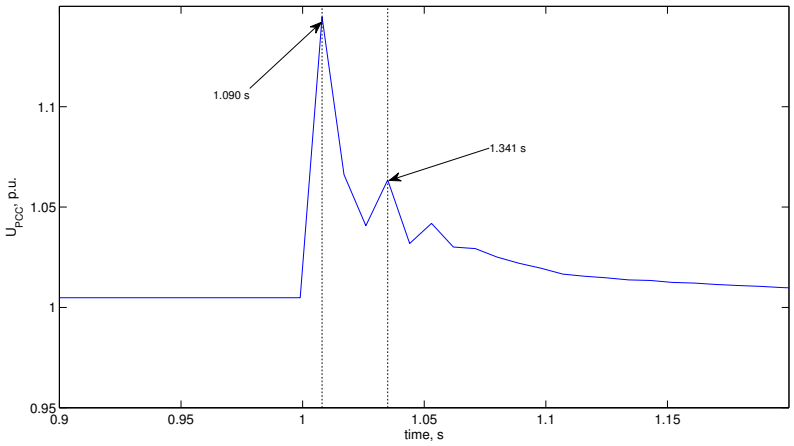

Figure 4.12: Enlarged oscillations of the system with modified controller

The stability of the modified system against the reference change can be confirmed by the fact, that the used power ramp has been implemented by the parametric event, which is carried out by the change of active power reference from 0.1 to 1 p.u. The obtained smooth voltage profile speaks for the system stability against the reference change. Therefore, the modified system is considered to be asymptotically stable.

4.4 Transient Stability

The system has achieved excellent performance in terms of transmitting capacity and small-signal stability, which has been previously constrained, according to for some published works, like in [5, 7, 34–38], which do not include the study of the transient behavior of the modeled systems. However, the research findings, which investigate the behavior of the low SCR connected WPPs, report unsatisfactory WPPs performance after faults clearing, for example references [3, 8] report slow voltage recovery after faults, which might result in grid codes requirements violation, while references [4,6] observe oscillatory instability after the fault clearing. Both are unacceptable in terms of power system stable operation. Therefore it is crucial that the designed system stays stable during the large disturbances, which means, that transient stability analysis has to be carried out within the thesis scope of study.

In order to determine the transient stability, the most severe disturbance test have to be carried out. The 3-phase ground fault was selected. Even though only around 5% of all faults account on 3-phase-to-ground faults [50], they result in highest fault current and are considered to be the most severe disturbances in the system. Moreover, as far as the used models are positive-sequence models [18], they are not purposed for calculation of unsymmetrical faults. Therefore, 3-phase short circuit to ground was applied. The selected SC location is shown on figure 4.13 is the Bus Z2, which can be considered to be ‘the bottleneck of the system. Tripping of circuit breakers, clearing short circuit at Bus Z2 will lead to further decrease of the SCR at the PCC from 1 to 0.9, which might enhance the severe effect of the fault and have unpredictable consequences on the voltage recovery.

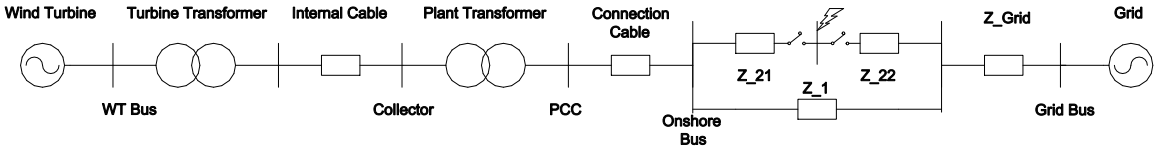

Figure 4.13: Fault location and tripping circuit breakers

The following sequence of the simulation events represent the power system contingency in order to simulate the worst case fault scenario, the events are summed up in table 4.6 and they are displayed on figure 4.13

Table 4.6: Simulated events

DSL Event	Time, s	Object	Comments
Short-Circuit Event	15	Bus Z2	Fault resistance = 0.3 Ω
Switch Event	15.25	CB 21	Circuit breakers 21 and 22 open,
Switch Event	15.25	CB 22	clearing the fault
Short-Circuit Event	15.3	Bus Z2	Fault clearing
Switch Event	15.6	CB 21	Circuit breakers 21 and 22 close,
Switch Event	15.6	CB 22	recovering system configuration

It is known, that the longer is the fault duration, the higher and the worse are the consequences for the network [51]. Therefore the duration of the short circuit was set to 0.25 seconds, which corresponds to the maximum fault duration, according to LVRT requirements [29]. The fault impedance is selected to be relatively small, as it would result in more severe effect on the system and the value was set to 0.3Ω resistive, the value is dictated by the typical power system factors, defining the fault impedance, for example the high-voltage towers resistance [52]. The reconnection of the CBs occurs in 0.35 seconds after the fault clearing, representing the dead time of the autorecloser. The relay manufacturers are always aiming to minimize the reclosure time, as it results in minimizing fault consequences for the system; however the dead time has a minimum threshold of 0.3 seconds after CB disconnection due to the necessity to eliminate the risk of excessive ionization at the fault location causing the reclosure to fail [53]. The voltage recovery time is limited to 3 seconds by the LVRT requirements of the grid codes - within this time the PCC voltage has to return to its steady-state limits [29].

After the first attempt to simulate the fault the system blacks out at the moment the disturbance is applied, which speaks for the inadequacy of the controller behavior during the UVRT mode. Therefore, the key settings of the UVRT have been modified. It is known, that the Q controller contains 3 possible UVRT control modes, depending on the reactive power injection during the voltage dips, and optionally for the post-fault operation. The modes are [18]:

1. Voltage dependent reactive current injection
2. Reactive current injection controlled as the pre-fault value plus an additional voltage dependent reactive current injection
3. Reactive current injection controlled as the pre-fault value plus an additional voltage dependent reactive current injection during fault, and as the pre-fault value plus an additional constant reactive current injection post fault

The initial setting of the UVRT mode was 1. However the mode does not perform well in the weak grid, while mode 2 and 3 perform equally well in response to the SC. The reason could be the fact, that for the modes 2 and 3 voltage dependent current injection is a minor portion additional to the fixed pre-fault value Updating UVRT mode enabled the simulations to converge, however, with a voltage spike of 2.75 p.u. occurs when the fault is cleared.

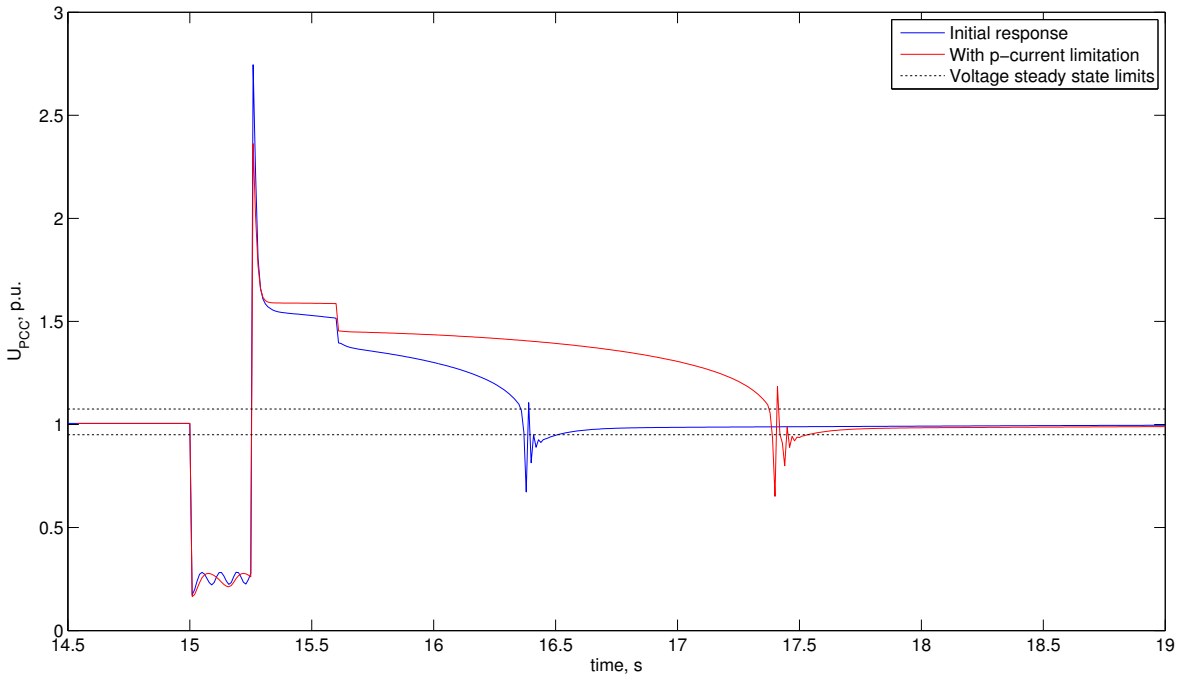

Figure 4.14: Voltage profile at the PCC, as a result of SC fault at Z2 bus

The blue line on the figure 4.14 shows the voltage at the PCC during the fault. It is observable, that oscillations take place during the fault period, which can be caused by the current injection by the turbine. An high voltage overshoot is observable at the moment, following the fault clearing. The high magnitude can be explained by the fact, that the clearing took place, when the turbine was injecting the currents into the fault location, initiating the spike. Further voltage step down is explained by the reconnection of the CBs, and finally the short oscillations at the time period [16.25-16.5] seconds are conditioned by the fact, that the turbine voltage has entered its deadband, therefore the UVRT flag, shown on figure 3.6 is switched off and the voltage control is being performed according to the normal operating conditions. In order to minimize the overshoot, relevant control parameters in the WT control block have been modified:

- The maximum active power rate ramp has been set to $0.2 p.u./s$. As it was discovered, that the smaller the ramp rate is, the smaller is the voltage overshoot [4]. However, the ramp rate cannot be infinitely small due to the grid codes limitations [29], therefore it was decided to stick to the lowest admissible value.
- Maximum reactive power injection during dip have been limited to 0.75 p.u., as the previous value of 1.2 p.u. resulted in excessive reactive power injection and high voltage overshoot at clearing.

- Maximum reactive power injection has been set to 1 p.u.
- Post-fault reactive current injection has been set to 0, as additional reactive power injection after fault clearing is only enhancing the voltage overshoot. By setting this value to zero, the after-fault voltage will stay at pre-fault level.
- Additionally in the Current limitation model, the lookup tables have been set in a way, that for the zero voltage active current injection is zero.

As a result of the above-mentioned means, the overshoot have been reduced to the value of 2.3 p.u. The value is still very high, however, what is peculiar is that the post-fault behavior of the PCC voltage is different from the one, which have been previously observed by the literature. Voltage oscillations and slow voltage recovery have been reported, but on the contrary the above-performed simulations result in fast voltage overshoot, which have not been observed earlier. The essence of the issue is of a dubious nature:

1. The numerical peculiarities of the models or the solver might result in voltage spikes [54]. That possibility is mentioned in the IEC61400-27-1: Reactive power spike, which might appear when the voltage recovers is mainly caused by numerical effects in the simulations [18].
2. The large amount of cable shunt capacitance is a source of reactive power, it is included into the modeled system, but in the previous research findings it has been neglected or compensated. In the normal operating conditions the amount of reactive power, produced by the cable is completely absorbed by the grid inductance, but in case of faults the reactive power flow might reverse its direction. The result of a reactive power injection into the bus is the voltage increase, which might explain the overshoot.

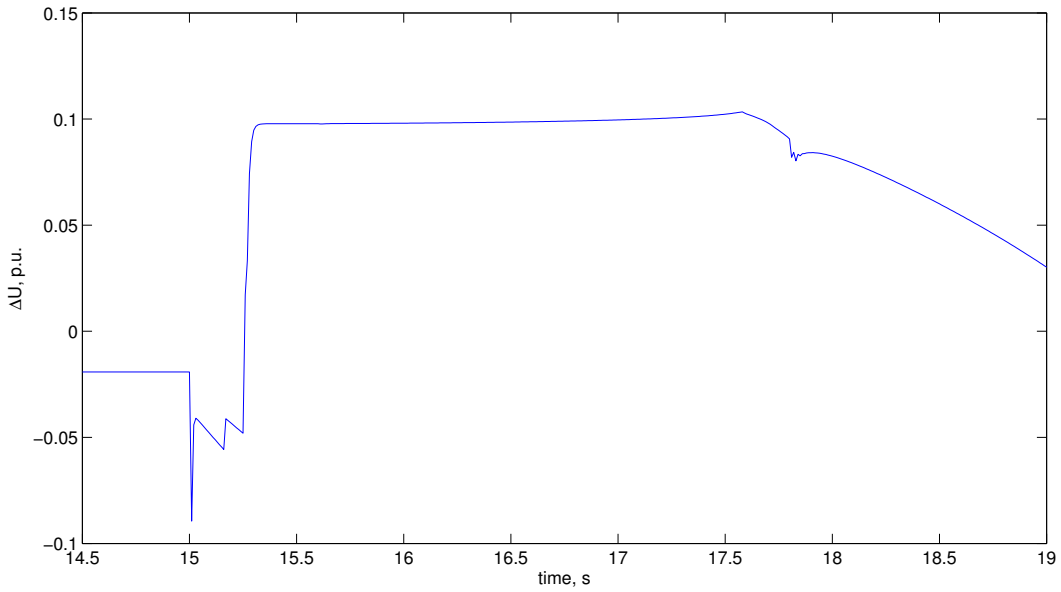

Figure 4.15: Voltage difference between the PCC and Offshore bus during the fault

The reason of the observed phenomena can lie in one of the described factors or their combination. Due to the absence of alternative models/software, there is no opportunity to check the hypothesis 1, however the second one can be checked. It is known, that the direction of the reactive power in the cable is dictated by the voltage difference between the buses, namely the flow is directed from the bus with lower voltage to the bus with higher voltage. In normal operating condition the voltage at the PCC is higher, than at the Offshore bus, ensuring the reactive power flow from the PCC into the grid. However in the contingency condition the difference may change. Taking into account the large amount of reactive power potentially available from the cable it was decided to check the Q flow direction. Therefore the difference between the voltages for the entire duration of the simulation have been plotted, it can be seen on figure 4.15.

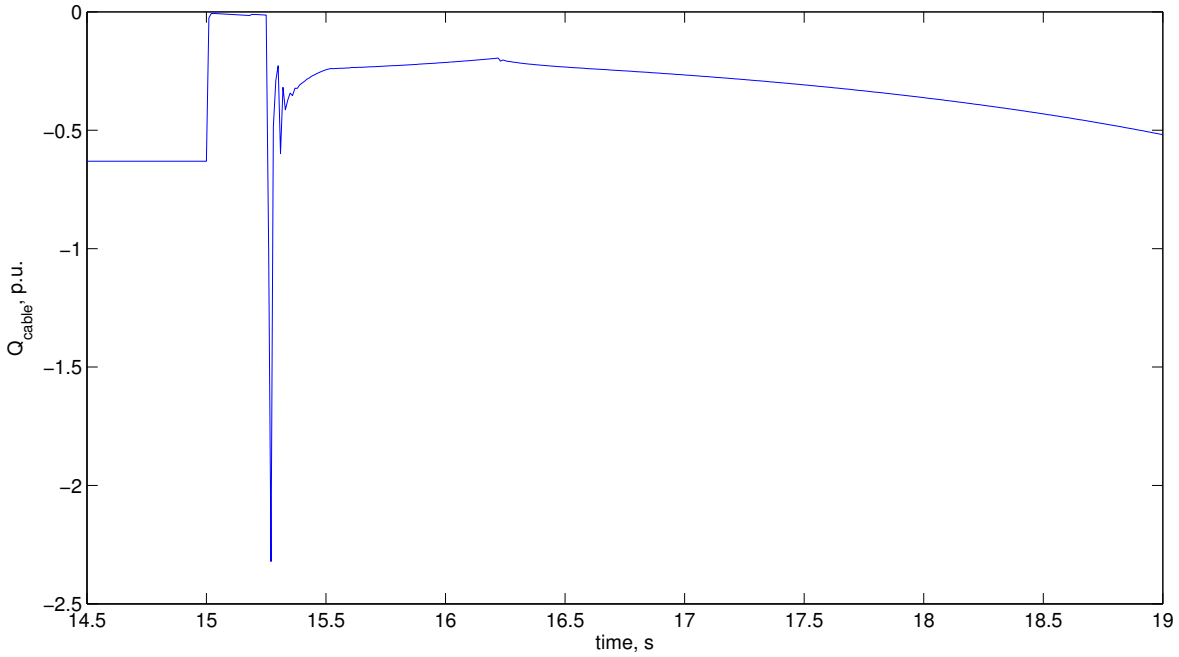

Figure 4.16: Injected reactive power

It can be concluded, that the reason of the arising high voltages lay in the Q, injected by the cable. The problem have not been faced often before, as most of the researched references are using the simplified modeling approach, neglecting the shunt capacitances of the cable. Therefore, they do not include the considerable amount of reactive power, which is being injected by the cable. The figure 4.16 demonstrates the reactive power, injected by the cable into the PCC. Therefore it was concluded, that the occurring voltage spike is not conditioned by the simulation effects, but it is purely due to the designed system topology. Since the cause of the problem lies in the system topology, the solution must be also based on the modification of the system configuration. As far as it is obvious that the considerable amount of the shunt capacitances result in voltage spike, while their absence result in insufficient voltage recovery, therefore the consequent solution is to introduce limited reactive power compensation. It has been proven, that due to certain grid codes limitations it is impossible to eliminate the compensation completely, for example, due to the limitations of the Q limits in the normal operation mode, depicted on figure 3.8 and due to the steady state voltage limitations; therefore reduced compensation is an alternative mean. The value of the reactive power compensation must be selected according to the balance of the two factors:

- The value must be large enough to compensate the reactive power, injected by the cable after the fault clearing and causing the voltage overshoot, but not completely compensating in order to avoid slow voltage recovery.
- Taking into account the fact, that the necessity of reactive power compensation varies, depending on the turbine active power output, the value of shunt compensation must be small enough in order not to demand additional reactive power from the turbine at high active power outputs

As an example it was decided to include shunt offshore compensation non-switchable, 0.2 p.u. reactive power, then the same events, as described by the table 4.6 have been applied. The final view of the voltage profile as the response to the short circuit is shown on figure 4.17. The figure has the same limits, as the previously shown figure 4.14, therefore it can be seen, that the transient performance of the system has been improved drastically: the voltage overshoot was considerably reduced, the voltage returns to its steady-state limits much faster and there are no more oscillations, occurring when the UVRT flag goes off. Therefore it was confirmed, that reducing the reactive power compensation for the connection cables is a promising method for improving the transient performance of the low SCR connected Wind Power Plants.

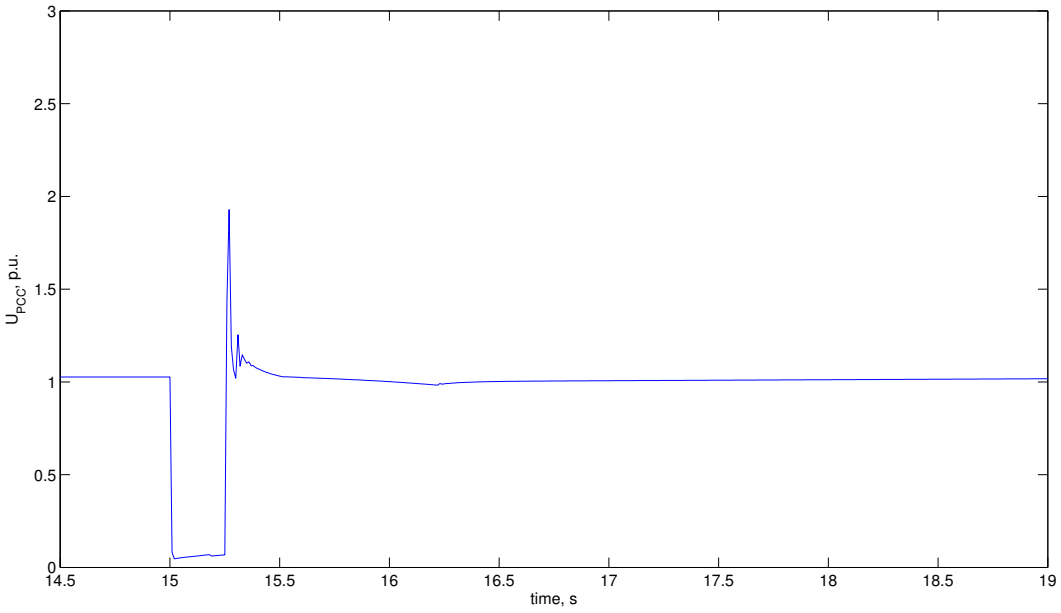

Figure 4.17: Voltage profile at the PCC, as a result of SC fault at Z2 bus, reduced Q compensation

The modified system demonstrates much better results, than the previous ones. The voltage overshoot has decreased to 1.9 p.u. and the voltage profile at the PCC and WT buses are within the admissible limits: the PCC satisfies the grid codes requirements and WT bus satisfies the protection requirements. Therefore it was concluded, that the transient performance of the turbine, connected to a week grid can be modified by adjusting the shunt compensation.

The down side of the solution is that the turbine has to inject certain amount reactive power during the full active power output. It is due to the fact, that the non-switchable compensation have been used. Solution could be STATCOM, however, it is a costly solution and demands additional tuning in

order to achieve good performance. Therefore, suggested alternative is the application of the variable shunt reactor with a built-in tap changer, for 132kV system it would have the regulation range $R = \frac{Q_{min}}{Q_{max}} \approx 0.375$ [55], therefore, for the 0.2 p.u. of maximum compensation, which is needed when the turbine has its maximum power output, the minimum value would be 0.075, which takes place when the active power output is at its maximum.

In order to conclude, that the proposed solution is effective, it is necessary to carry out the full cycle of the simulations again. First, the power ramp from 0 p.u. to 1 p.u. have been applied.

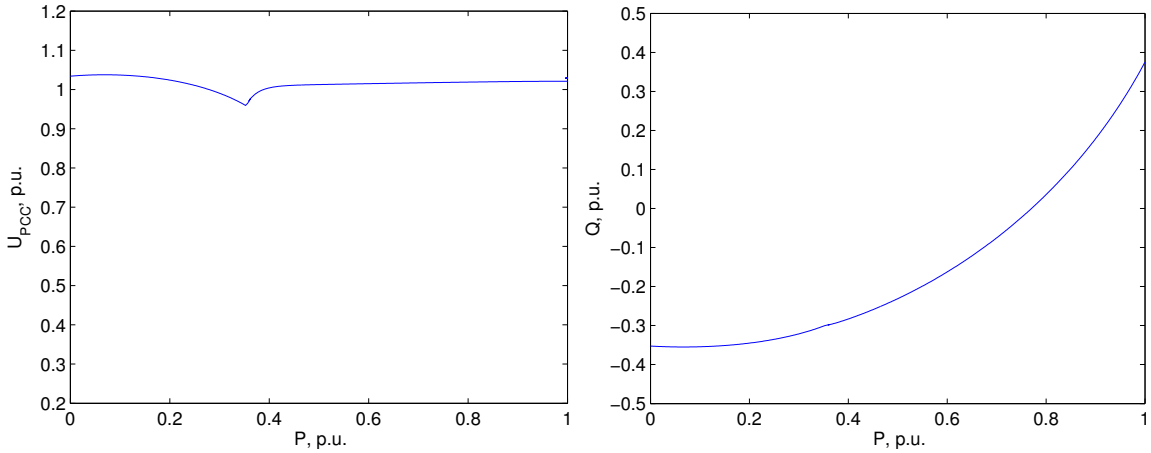

(a) (b)

Figure 4.18: PV (a) and PQ (b) curves for the final system model

PQ curve has a typical shape for the voltage control mode, corresponding to what has been explained in section 4.0.1, while the PV curve is of a somewhat unusual shape: the curve is originally decreasing along the active power injection increases, however at certain moment of time, after having reached a certain value, it starts to increase. That behavior can be explained by the converter currents limitations.

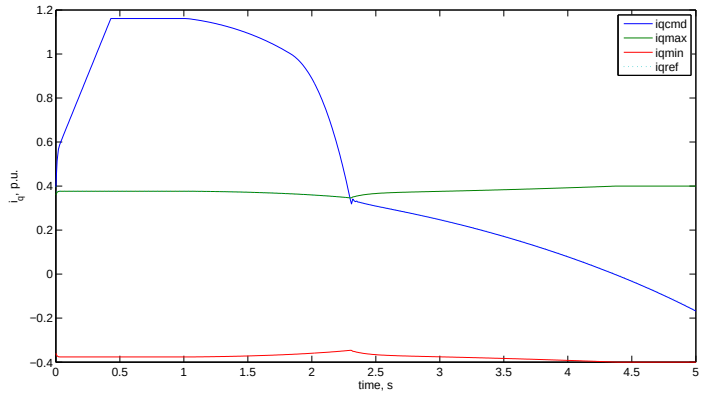

Figure 4.19: Converter q-current, its limits and reference along the power ramp

As it is seen on figure 4.19, up to the time moment t=2.3 s, the command value iqcmd, which is the output of the Q control model, shown on the figure 3.6 was exceeding the q-current limit iqmax, which has been set in the current limitation model as seen in the table 3.5. the q-current reference was sticked to its upper limit. Therefore the total injected Q was not sufficient to maintain the voltage at its setpoint, but after t=2.3 s the q-current command meets the maximum limit and the q-current reference, recovering the voltage to its setpoint.

5 | Effect of the SCR and X/R Ratio on the Controller Performance

The previous chapters have been considering only two system models, namely a weak grid with SCR 1 and a strong grid of SCR 5, both having the same X/R ratio, which has been set to 10. This chapter has been added for the sake of consistency, as it addresses the voltage response to SCR and X/R parameters variation on a wide scale. The main purpose of this study is to reflect those parameters influence in the control frame.

5.1 Control Refinement

Controllers tuning is a crucial step in ensuring stable operation of the grid-connected WPP. The controller gains updates, which has been carried out within the section 4.2 was a rough approximation of the settings, which would be applicable specifically for the weak grids application, because the original settings, as it is common for the WT controllers, have been tuned, assuming normal grid connection condition (i.e. SCR higher, than 3) [4]. However, in reality the controllers tuning is a sophisticated procedure, and special loop tuning techniques are being applied by the industry, instead of the trial and errors method [49]. There are various controller tuning techniques, like modulus optimum, symmetrical optimum, technical optimum etc. Each of them aims to achieve maximum stability and performance via different objective functions. The choice of method depends on the system peculiarities, i.e. presence of dominant time constant, amount of delays in the system, as well as on the objective function, like for example, maximum flatness of the Bode plot etc. The common about the various tuning method is that they are all using the same voltage loop transfer function, as shown on figure 5.1.

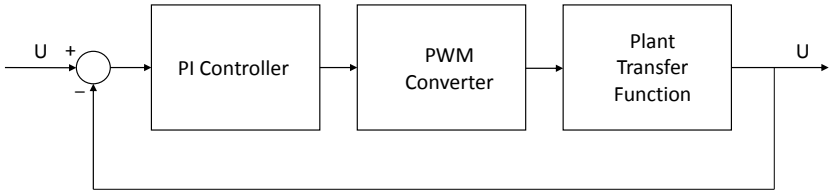

Figure 5.1: Block diagram of the system transfer function

The PI controller transfer function is well known and is represented as, where K_p is a proportional gain and T_i is an integral time constant.:

$$G_c(s) = K_p \cdot (1 + \frac{1}{T_i s}) = K_p \cdot \frac{T_i s + 1}{T_i s} \tag{5.1}$$

PWM is traditionally considered as an ideal transformer with a time delay [49], therefore its transfer function can be expressed as follows, T_{switch} being the converter switching time constant.:

$$G_t(s) = \frac{1}{1 + 2 \cdot T_{switch} s} \tag{5.2}$$

The transfer function of the plant is not a straightforward matter, it can be treated in different ways. Some models include the impedances of the converter, its DC-link and filter, which is, although, more widespread for the HVDC application [56]. Another definition of plant transfer function for HVAC connected WT converters is defined as the impedance between the converter and the point, where the control takes action [57], which in the studied case is the PCC. However, accepting this expression of the plant transfer function it is obvious, that the system on the right side of the PCC is not included in the transfer function. This is not an issue for the high SCR values, as the grid does not have significant effect on the PCC voltage, however for the weak grid condition the voltage is going to be affected. Therefore it has been decided to include an SCR-dependent gain into the plant transfer function.

5.2 SCR Influence

In order to determine the influence of the SCR onto the PCC voltage, the corresponding test system have been established in DIgSILENT PowerFactory. The originally used system from the figure 3.1 has been modified: WPP, as well as an entire part of the system, left of the PCC remains unchanged, while the Thevenins impedance of the grid is represented by 10 parallel impedances, having the same impedance value: 0.1+i1 p.u., the obtained system look like it is shown on figure 5.2.

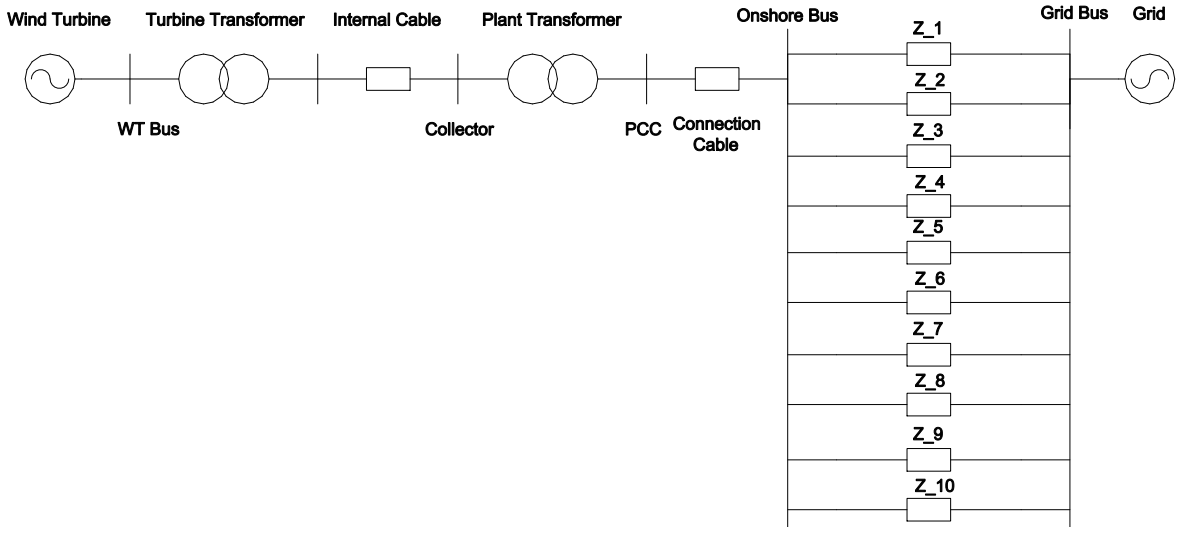

Figure 5.2: The designed system for the voltage dependence of SCR detecting

After initialization at full active power output, during the dynamic simulations, with the 10 seconds interval, the parallel impedances have been disconnected one by one, resulting in stepwise decrease of SCR. Due to the fact, that the PCC voltage setpoint remains constant U_{PCCref}=1p.u. and that the variable in the controller voltage loop is the WT voltage, parameter of interest in the test system is

the voltage at the WT, shown in figure 5.3.

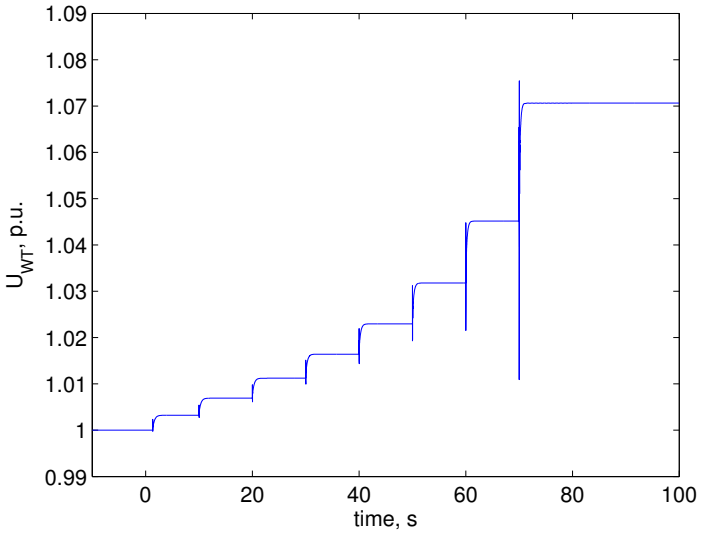

Figure 5.3: Voltage response to the stepwise increase in grid impedance

The fact, that the voltage drop characteristic was enabled in the Q control mode, has certain consequences for the simulation results:

- The WT voltage is being tracked, as the PCC voltage stays unchanged throughout the simulation, due to control actions. If the drop is disabled, the WT voltage stays constant and the PCC voltage changes stepwise.
- It is observed, that the WT voltage increases during the simulation, that is conditioned by the the necessity to keep the voltage at the PCC at the 1 p.u. level. When the drop is disabled, the PCC voltage decreases stepwise.

Even though the simulations have been performed dynamically, in order to take into account the controllers performance, the value of importance is the steady state voltage. The RMS simulations in PowerFactory are, in their nature, a sequence of successive load flow solutions, therefore, the corresponding steady-state values of the voltages can be obtained through the interpolation of the discrete signal,the result is shown on figure 5.4.

In order to obtain more accurate dependence between SCR and voltage it has been decided to calculate SCR at the WT bus, using the formula:

$$SCR_{WT} = \frac{1}{Z_{WT-PCC} + \frac{1}{\sum_{i=1}^{n} \frac{1}{Z_i}}} \tag{5.3}$$

After carrying out interpolation, the polynomial approximation method has been applied in Matlab in order to obtain the function, expressing the voltage variation through SCR.

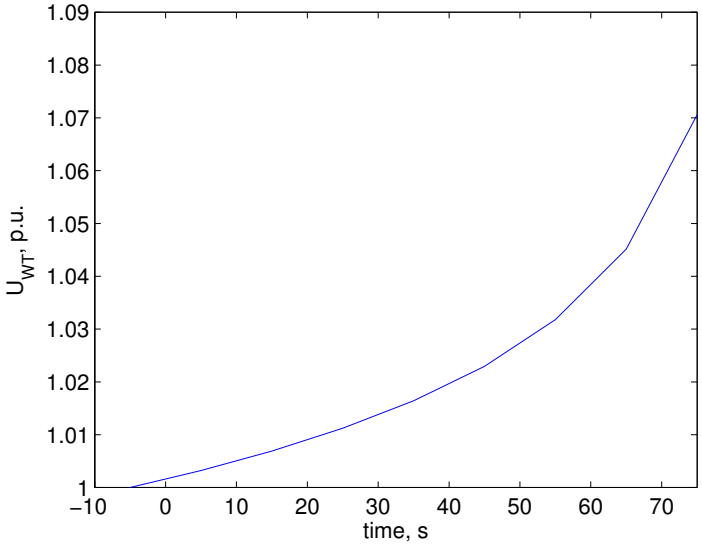

Figure 5.4: Interpolated voltage response to the increase in grid impedance

The obtained dependence has been derived:

$$U_{WT}(SCR) = 0.0067 \cdot SCR^2 - 0.063 \cdot SCR + 1.1142 \tag{5.4}$$

The above equation has been used in order to calculate WT voltage, as a function of the SCR. The obtained values have been compared to the simulated ones.

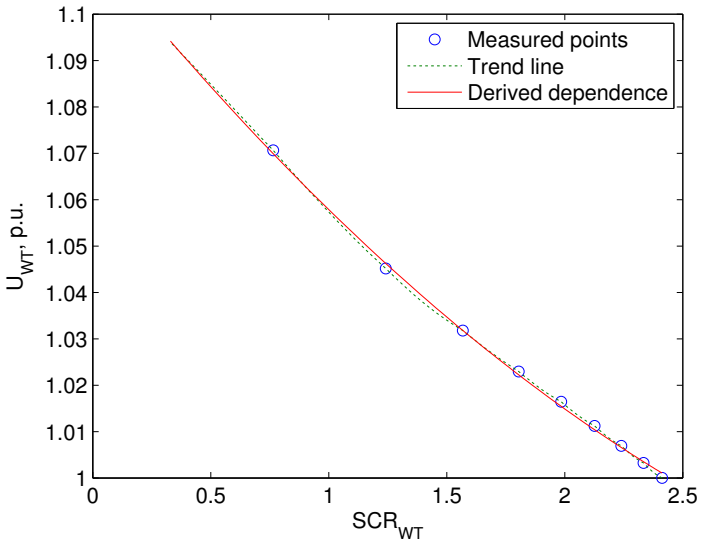

Figure 5.5: WT voltage as a function of the SCR at the WT bus

In order to evaluate the accuracy of the fit, the difference between the two curves have been calculated

and plotted along all the SCR values, as shown on figure 5.6

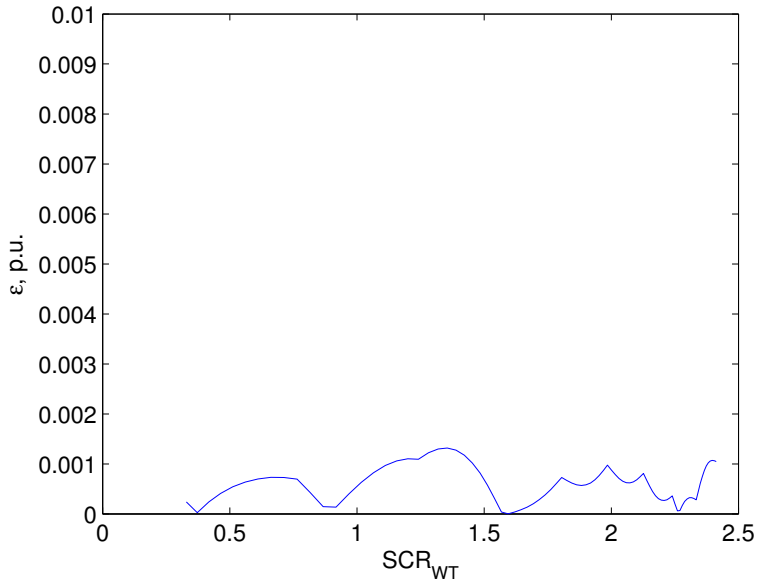

Figure 5.6: Error between the calculated and simulated values of the voltage

The obtained curve gives a good fit (error is less, than 0.5%) for the SCR values up to 2.5, which corresponds to the SCR at the PCC:

$$SCR_{PCC} = \frac{1}{\frac{1}{SCR_{WT}} - Z_{WT-PCC}} = \frac{1}{\frac{1}{2.5} - 0.25} = 6.67 \tag{5.5}$$

At higher SCR values, the voltage gain equals to unity.

The U_{WT} in the expression 5.7 can be treated as follows: taking into account, that the initial value of the U_{WT} was 1 p.u., its dependence of the SCR can be expressed as:

$$U_{WT}(SCR) = U_0 \cdot K_{G(SCR)} \tag{5.6}$$

where U_0 is the initial value of the WT voltage on condition of strong grid, i.e. SCR>7. Normally the value is 1 p.u. $K_{G(SCR)}$ is the SCR dependent gain, expressed by the expression, derived from 5.7:

$$K_{G(SCR)} = 0.0067 \cdot SCR^2 - 0.063 \cdot SCR + 1.1142 \tag{5.7}$$

The obtained gain block can be added into the transfer function of the system, which is going to be used for the controllers tuning refinement. The advantage of this method is that the standard tuning techniques can be used for controllers tuning, the only refinement, that is needed is the system transfer function, which will have the following look:

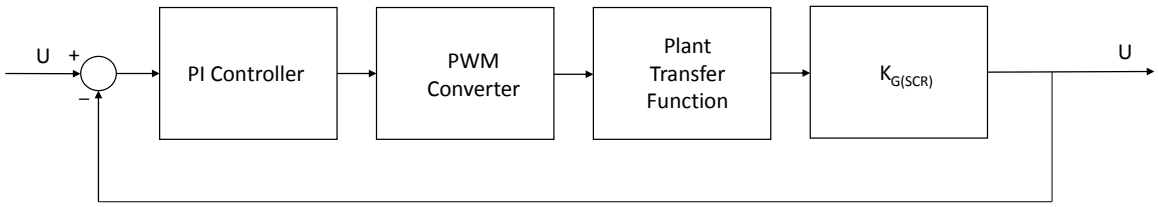

Figure 5.7: Block diagram of the modified system transfer function

5.3 X/R Ratio Influence

Previously it has been investigated in the academia, for example in reference [58], that the network impedance phase angle influences the voltage deviation response to the active power injection. In order to address the phenomena, the notation X/R ratio is widely used. The same method can be used, when it is desired to include X/R ratio into the function. Analogous experiment has been carried out for the following X/R ratios: 0.1, 1, 5, 10, 20, 50, 100. Certain limitations occurred, as for the X/R ratios higher, than 20, the system didn't converge for the SCRs, lower, than 1.5. The obtained 3-dimensional array of data represents the U_{WT} dependence on $SCRWT$ and X/R ratio of the grid. Expression 5.6 still holds and similarly, U_{WT} value can be treated as $K_{G(SCR)}$. The only difference is that instead of the expression 5.7, the table-lookup method can be used. The interpolated 3-dimensional dependence is represented by figure 5.8.

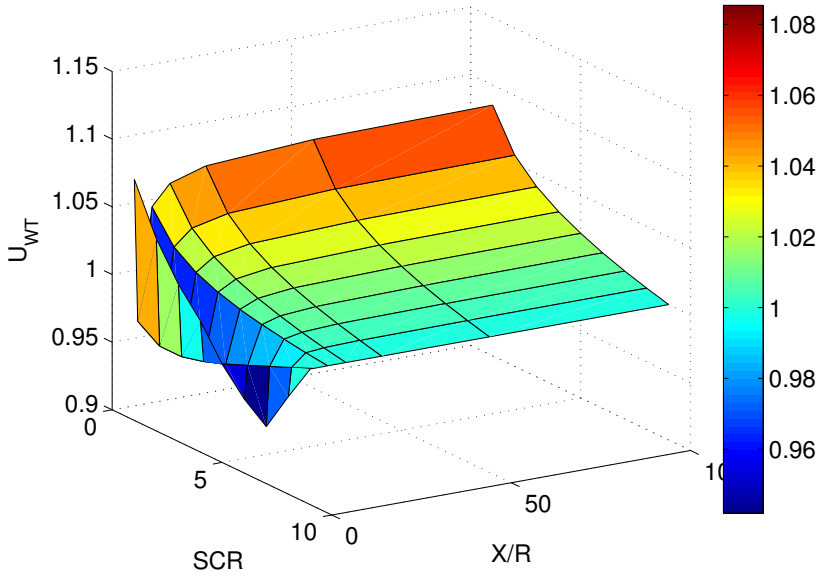

Figure 5.8: Dependence of U_{WT} on SCR and X/R ratio

There is unclear region in the area of low X/R ratios, an insignt into the essence of such performance has been taken. For the investigated case of weak grid (SCR=1), voltage control mode the X/R ratio has been varied from 1 to 100 and the maximum transferable active power has been measured.

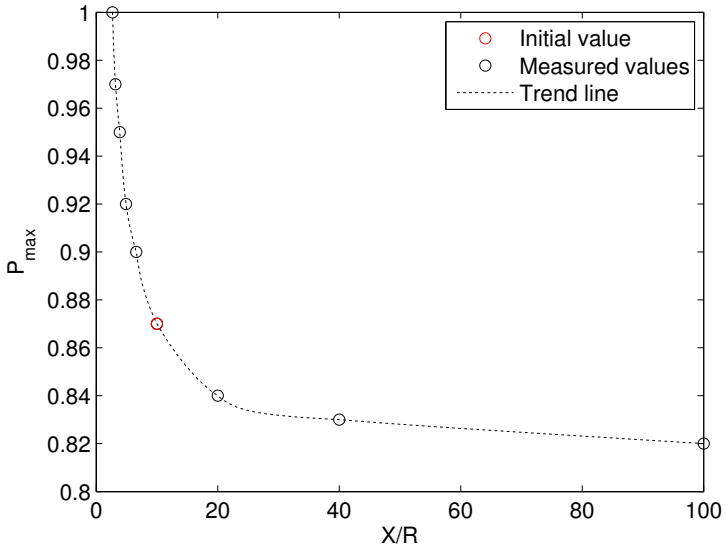

Figure 5.9: Maximum transferable active power as a function of X/R ratio

It can be observed, that the smaller X/R ratio, the higher is the maximum transferable active power. In order to investigate feasibility of decreasing the X/R ratio (through increasing the series resistance), the grid losses for all the X/R ratios have been defined.

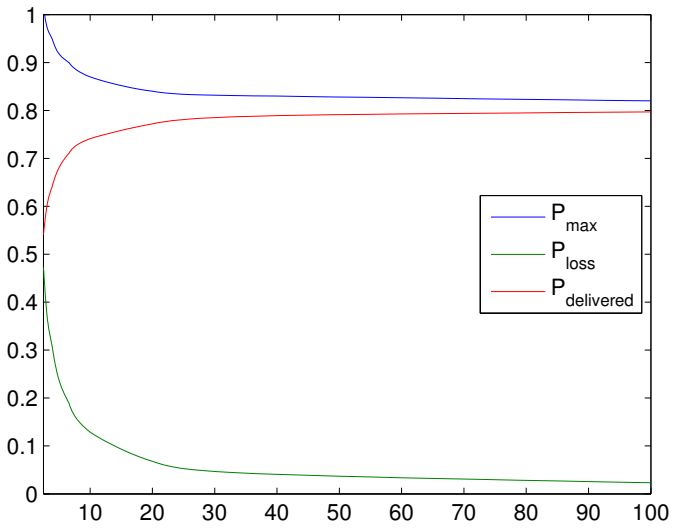

Figure 5.10: Powers for all the X/R cases

From the figure 5.10 it can be seen, that even though the maximum transferable active power is higher for lower X/R ratios, the resulting system losses increase with a higher slope, then P_{max}, resulting in total lower delivered power, therefore the investigated approach can not be accepted as feasible.

6 | Conclusions

The overall results of the work are considered as positive due to fulfillment of the stated objective functions. The observed phenomena have been explained prom the power system point of view and the solutions have been proposed and tested. The successful outcome of the work can be evaluated due to the achievement of the measurable goals:

- The steady state connection of the one per unit active power to a grid with the unity short circuit ratio has been successfully carried out. The system operates well along the entire range of active power output, as the system operates with the PV curve of a high flatness.
- Small signal stability of the system has been achieved. The oscillations, which occur as a results of small disturbances have negligible magnitude and are damped fast.
- A variety of transient instabilities has been avoided: the system, unlike the similar systems, designed by the industries does not initiate uncontrolled oscillations or low voltage collapse/insufficient voltage recovery.
- The system fulfills the design grid codes requirements, making prospectives for further studies and successful implementation.

Certain findings have arisen throughout carrying out the thesis work. Some of them have relation to the study objective function, while the others have been derived additionally, as a result of the insight taken into the nature of the weak grids:

- The first observed results conclude, that the voltage control mode performs considerably better, compared to the reactive power and power factor control modes due to higher limits of reactive power injection. Additional advantages of the mode is that the voltage at the point of common coupling is always kept at its setpoint, and the control tuning is more straightforward due to the presence of one PI control loop. All above mentioned is speaking for the prospects of the voltage control mode application for the wind turbines, connected to the weak grids.
- It was proven by the preliminary studies, that for the power system modeling, dealing with low short circuit ratio connection of wind power plants, the simplified conventional modeling of the transmission line, where the line is represented by the series inductance only is not relevant. On the contrary it is essential to include the shunt capacitance in order to reach the minimum possible short circuit ratio.
- For the load flow studies, dealing with full-converter wind turbines connection to weak grids it is essential to supplement the load flow studies with the dynamic simulations in order to include the possible limitations, introduced by the controllers performance.
- The voltage-dependent reactive power injection undervoltage ride-through support mode for wind turbines, which is required by some grid codes, has been proved to be the least effective

on conditions of low short circuit ratio connection and to have highly negative effect on system robustness against the short circuit faults. While the fixed value with d-current zero during the fault have achieved successful implementation.

- When wind turbines are connected to weak grids by the cables, the amount of the reactive power compensated is crucial for the wind power plant operation. The reactive power compensation has been proven to be not necessary during high active power output, because the generated reactive power is being completely absorbed by the week grid. However, completely eliminating the compensation would have highly negative effect on the system transient performance, namely, high voltage overshoots after fault clearing. That eliminates the problem of the slow voltage recovery after faults, as the cable is injecting its reactive power into the point of common coupling, increasing the voltage, however, the resulting overshoot value is not acceptable. Furthermore, for the low active power outputs, the reactive power from the cable can be absorbed by the wind turbine converter. Therefore, the coordination of the optimal value of the reactive power compensation has to be defined on case-by-case basis, which would result in minimum voltage overshoot after fault clearing and at the same time would not demand least reactive power production from the turbine at low active power outputs.
- Due to the fact, that the grid impedance has significant effect on wind turbine/point of common coupling voltage, the accuracy of the conventional system transfer function, used for the controller tuning purposes, on condition of week grid can be improved by the inclusion of the short circuit ratio dependent gain.

To conclude, this project shows that connection of large wind power plants to weak grids demands demands specific approach in terms of simulations, reactive power compensation and controllers tuning. The thesis has not proven it to be impossible to connect a wind power plant of one per unit capacity to a connection point with unity short circuit ratio.

This work contributes to better understanding of the nature of the high impedance grids, pointing out the main features and operation principles. However, the findings of the work have naturally caused further questions and prospective fields for the research. Among those:

- The findings of the work, which have resulted in successful connection of the one per unit capacity wind power plant to a grid with unity short circuit ratio can be verified by a case study. The obtained recommendations for the control mode selection, controller settings and portion of the reactive power compensated can be, for example implemented with a different wind turbine model. The voltage overshoot has to be regulated by varying the amount or reactive power compensated in order to achieve the design requirements.
- The exact implementation and limitations, introduced by the low active power output are still to be investigated. Grid codes state their demands on condition of maximum active power output, while the possible faults occurring at low active power output might have unpredictable consequences.
- Verification of the findings regarding the short circuit ratio dependent gain is needed: transfer functions and calculated gains in order to compare them with the ones, obtained with the short circuit ratio term included. That topic can be addressed in further works, which concentrate on controllers tuning with application of the known loop tuning techniques.

Bibliography

[1] N.-E. Clausen, *Planning and development of wind farms: Environmental impact and grid connection*, DTU Wind Energy, 2013

[2] G. Corbetta et al., *The European offshore wind industry - key trends and statistics 2013*, A report by the European Wind Energy Association, 2014

[3] R. Piwko et al., *Integrating Large Wind Farms into Weak Power Grids with Long Transmission Lines*, IEEE International Power Electronics and Motion Control Conference, 2006

[4] S.-H. Huang et al., *Voltage control challenges on weak grids with high penetration of wind generation: ERCOT experience*, IEEE Power & Energy Society General Meeting, July 2012

[5] R. Reginato et al., *Analysis of Safe Integration Criteria for Wind Power with Induction Generators Based Wind Turbines*, IEEE, 2009

[6] J. W. Feltes and B. S. Fernandes, *Wind Turbine Generator Dynamic Performance with Weak Transmission Grids*, IEEE, 2012

[7] V. Diedrichs et al., *Control of Wind Power Plants Utilizing Voltage Source Converter in High Impedance Grids*, IEEE Power & Energy Society General Meeting, San Diego, California, July 2012.

[8] F. Sulla et al., *Wind turbines voltage support in weak grids*, IEEE Power and Energy Society General Meeting 2013 , July 2013

[9] E.ON Netz GmbH, *Grid Code High and Extra High Voltage*, Bayreuth, Germany, 2006

[10] P. Navarro-Perez, R.B Prada, *Voltage collapse or steady state stability limit*, Proceedings of the International Workshop on Bulk Power System Voltage Phenomena: Stability and Security, Maryland, USA, 1991

[11] E. Muljadi et al., *Short Circuit Current Contribution for Different Wind Turbine Generator Types*, IEEE Power & Energy Society General Meeting, Minneapolis, Minnesota, July 25-29, 2010

[12] J. Bech, *Wind turbine control for a weak grid by reducing active power output* , U.S. Patent: 20130300118 A1, 2013

[13] J. L. Thomason et al., *The properties of glass fibers after conditioning at composite recycling temperatures, Compos. Part A*, Appl. Sci. Manuf., vol. 61, 2014

[14] P. E. Morthorst et al., *Wind economics* , DTU International Energy Report 2014, DTU National Laboratory for Sustainable Energy, 2014

[15] H. H. Larsen and L. S. Petersen, *Wind energy drivers and barriers for higher shares of wind in the global power generation mix*, DTU International Energy Report 2014, DTU National Laboratory for Sustainable Energy, 2014

[16] E. Tedeschi, lecture slides for the course *Power Electronics in Future Power System*, Norwegian University of Science and Technology, 2014

[17] Y. Ashkhane, *A new approach to improve voltage stability in a network with fixed speed wind turbines*, 19th Iranian Conference on Electrical Engineering, 2011

[18] P. Sørensen et al., *IEC 61400-27 Electrical simulation models for wind power generation*, IEC, 2015

[19] J. Carroll et al., *Reliability comparison of DFIG drive train configuration with PMG drive train configuration in the first 5 years of operation*, Renewable Power Generation Conference, IET, 2014.

[20] O. Anaya-Lara, *Wind turbine and wind farm control and system integration*, lecture slides for ELK-12 Wind Power in the Norwegian Energy System, Norwegian University of Science and Technology, 2014

[21] T. Ackermann, *Wind Power in Power Systems, 2nd Edition*, Wiley, 2012

[22] A. Gavrilovic, *AC/DC System strength as indicated by short circuit ratios*, in Int. Conference on AC and DC Power Transmission, London, UK, 1991.

[23] T. Toftevaag, *Wind PowerGrid connection of wind farms*, lecture slides for ELK-12 Wind Power in the Norwegian Energy System, Norwegian University of Science and Technology, 2014

[24] P. Kundur, *Power system stability and control*, McGraw-Hill, 1994

[25] B. Kalyan Kumar, *Power system stability and control*, Department of Electrical Engineering, Indian Institute of Technology Madras, Chennai, India, 2004

[26] F. M. Gonzalez-Longatt, J. L. Rueda, *PowerFactory Applications for Power System Analysis*, Springer, 2014

[27] J. Bech, *Personal communication*, 3 July 2015

[28] P. Sørensen et al., *Modular structure of wind turbine models in IEC 61400-27-1*, IEEE, 2013

[29] *ENTSO-E Network Code for Requirements for Grid Connection Applicable to all Generators*, ENTSO-E AISBL, Brussels, 2013

[30] C. A. Rapp, master's thesis *Control of HVDC connected cluster of wind power plants*, Technical University of Denmark, 2015

[31] D. F. Opila et al., *Wind Farm Reactive Support and Voltage Control*, IREP Symposium - Bulk Power System Dynamics and Control, Buzios, 1-6 August 2010

[32] *Gamesa 5.0 MW Innovating for reliability*, Gamesa Corporación Tecnológica, S.A , 2005

[33] S. Navalkar,Lecture *Wind turbine design. Control of variable speed wind turbines*, Delft Center for Systems and Control, Delft University of Technology, 2014

[34] Y. Zhou et al., *Connecting wind power plant with weak grid - Challenges and solutions*, IEEE Power & Energy Society General Meeting, July 2013

[35] V. Diedrichs et al., *Operation of Wind Power Plants in High Impedance Grids. Loss of stability control for maximizing wind power vs. power quality*, The 11th International Workshop on Large-Scale Integration of Wind Power into Power Systems as well as on Transmission Networks for Offshore Wind Farms, Lisbon, 13-15 November 2012

[36] V. Diedrichs et al., *Wind Power Plants for Weak Grids based on Type IV Wind Energy Converters*, The 13th International Workshop on Large-Scale Integration of Wind Power into Power Systems as well as on Transmission Networks for Offshore Wind Farms, Berlin, 11-13 November 2014

[37] J. Garcia et al., *Fakken Wind Power Plant: a Case of Weak Grid Connection*, The 11th International Workshop on Large-Scale Integration of Wind Power into Power Systems as well as on Transmission Networks for Offshore Wind Farms, Lisbon, 13-15 November 2012

[38] W. Kuehn, D. Mueller, *Stability of VSC HVDC Connected Offshore Wind Power Plant at Low SCR*, The 11th International Workshop on Large-Scale Integration of Wind Power into Power Systems as well as on Transmission Networks for Offshore Wind Farms, Lisbon, 13-15 November 2012

[39] S. Engelhardt, A. Geniusz, *Method for Operating a Wind Turbine*, US2011/0006528 A1, Jan. 13, 2011

[40] M. L. Wittrock, *Loadflow Project*, 31730 Electric Power Engineering, DTU Elektro, 2013

[41] L. P. Lazaridis, master's thesis *Economic Comparison of HVAC and HVDC Solutions for Large Offshore Wind Farms under Special Consideration of Reliability*, Royal Institute of Technology, Stockholm, 2005

[42] T. Ackermann et al., *Evaluation of Electrical Transmission Concepts for Large Offshore Wind Farms*, Royal Institute of Technology, Stockholm, 2005

[43] P. Sørensen, *Personal communication*, 9 March 2015

[44] *DIgSILENT PowerFactory 15 User Manual*, DIgSILENT GmbH, 2015

[45] J. L. Rueda, Lecture slides for the course *Power System Dynamics*, Delft University of Technology, 2014

[46] N. D. Caliao, *Small-signal analysis of a fully rated converter wind turbine*, Journal of Renewable and Sustainable Energy, AIP Publishing, 2011

[47] *PWM Converter ElmVsc, ElmVscmono*, DIgSILENT PowerFactory Technical Reference Documentation, DIgSILENT GmbH, 2014

[48] Control Tutorials for MATLAB and Simulink, *Introduction: PID Controller Design*, Published with MATLAB R 7.14, 2012

[49] M. Molinas, lecture notes for the course *Power Electronics in Future Power System*, Norwegian University of Science and Technology, 2014

[50] V. Vadlamudi, *Control of VSC-HVDC for wind power*, lecture slides for the course *Power System Analysis*, Norwegian University of Science and Technology, 2014

[51] R. Nylen, *Auto-reclosing*, ABB Relays, Reprint from ASEA Journal 1979

[52] V. De Andrade, E. Sorrentino, *Typical expected values of the fault resistance in power systems*, IEEE Power & Energy Society Transmission and Distribution Conference and Exposition: Latin America, 2010

[53] Siemens Industry, Inc., *Reclosing applications - minimum reclosing time*, Siemens Industry, Inc., Wendell, NC, 2012

[54] P. Sørensen, *Personal communication*, 9 June 2015

[55] ABB AB Power Transformers, *ABB Variable Shunt Reactors*, ABB Shunt Reactors Applications, 2009

[56] C. Bajracharya, master's thesis *Control of VSC-HVDC for wind power*, Norwegian University of Science and Technology, Department of Electrical Power Engineering, 2008

[57] A. Constantin, doctoral dissertation *Advanced Modelling and Control of Wind Power Systems*, Institute of Energy Technology, Aalborg University, Denmark, 2009

[58] J. O. Tande , *Exploitation of wind energy resources in proximity to weak electric grids*, Applied Energy (Elsevier), 2000

[59] K. Hanson, *Application Guide for Static var compensators.*, Electricity Supply Board Ireland (ESB) System Operation Department, Dublin, November 1985.

Appendices

A Matlab Code for Per Unit Calculations

```
clc
clear all
close all

%General parameters
f=50;
w=2*pi*f;
S_base=100e6;
%base voltages for p.u. calculation in 3 voltage zones
%        WT | cable| PCC - grid
U_base=[3e3    33e3    132e3 ];
%zone impedances
Z_base=U_base.^2/S_base;

%equipment impedances

%WT and WPP transformers impedances in p.u.
Z_tr_pu=[0.1  0.12];

%Wind Farm internal cable
Z_int_cable=0.037+i*0.362;  %C=0.2uF/km
Z_int_cable_pu=Z_int_cable/Z_base(2);

%Z grid
Z21=i*0.1; Z22=Z21;
Z1=i*0.2; Z2=Z21+Z22;
Z_G=i*0.5;
Z_grid_pu=(Z1*Z2)/(Z1+Z2)+Z_G;
Z_grid=Z_grid_pu*Z_base(3);

%Cable to PCC as general impedance
Z_to_PCC_pu=i*0.2;
Z_to_PCC=Z_to_PCC_pu/Z_base(3);

%     tr1         internal cable        tr2         Line           Grid
Z_pu=[Z_tr_pu(1)    Z_int_cable_pu      Z_tr_pu(2)  Z_to_PCC_pu
    Z_grid_pu];

%calculation of SCR in per unit at different points
SCR_PCC=abs(1/( Z_pu(5)+ Z_pu(4)) )
SCR_grid_terminals=abs(1/Z_pu(5))
SCR_WTT=abs( 1/sum(Z_pu) )

%Local base parameters for input in PowerFactory
Z_tr_pf(1)=Z_tr_pu(1)*(U_base(2)/33e3)^2.*(125e6/S_base);
Z_tr_pf(2)=Z_tr_pu(2)*(U_base(3)/132e3)^2.*(110e6/S_base)
```

B Note on DIgSILENT PowerFactory

The content of this appendix has been provided by DIgSILENT GmbhH, the full text can be found in the reference [44].

B.1 Simulation tool

The calculation program DIgSILENT PowerFactory , is a computer-aided engineering tool for the analysis of transmission, distribution, and industrial electrical power systems. It has been designed as an advanced integrated and interactive software package dedicated to electrical power system and control analysis in order to achieve the main objectives of planning and operation optimization.

A basic function which uses a symmetrical steady-state (RMS) network model for mid-term and long-term transients under balanced network conditions.

The balanced RMS simulation function considers dynamics in electromechanical, control and thermal devices. It uses a symmetrical, steady-state representation of the passive electrical network. Using this representation, only the fundamental components of voltages and currents are taken into account.

Time-domain simulations in PowerFactory are initialised by a valid load flow, and PowerFactory functions determine the initial conditions for all power system elements including all controller units and mechanical components. These initial conditions represent the steady-state operating point at the beginning of the simulation, fulfilling the requirements that the derivatives of all state variables of loads, machines, controllers, etc., are zero. Before the start of the simulation process, it is also determined what type of network representation must be used for further analysis, what step sizes to use, which events to handle and where to store the results. The simulation uses an iterative procedure to solve AC and DC load flows, and the dynamic model state variable integrals simultaneously. Highly accurate non-linear system models result in exact solutions, including during high-amplitude transients. Various numerical integration routines are used for the electromechanical systems.

The process of performing a transient simulation typically involves the following steps:

1. Calculation of initial values, including a load flow calculation
2. Definition of result variables and/or simulation events
3. Optional definition of result graphs and/or other virtual instruments
4. Execution of simulation
5. Creating additional result graphs or virtual instruments, or editing existing ones
6. Changing settings, repeating calculations
7. Printing results

B.2 Used PowerFactory Elements

ElmGenstat

The Static Generator is an easy-to-use model of any kind of three or single phase static (no rotating) generator. Applications are:

- Photovoltaic Generators
- Fuel Cells
- Storage devices
- HVDC Terminals
- Reactive Power Compensators
- Wind Generators

Wind generators, which are connected through a full-size converter to the grid, can also be modeled as static generators, because the behavior of the plant (from the view of the grid side) is determined by the converter.

The number of parallel machines can be entered, as well as the MVA rating of a single generator. In general, the total MW and Mvar outputs of the static generator will be the dispatch of a single generator multiplied by the number of parallel machines. In the specific case of the Wind Generator category, the output will additionally be affected by the Wind Generation Scaling Factor of the zone to which it belongs.

Used as an aggregated WT model

ElmTr2

The 2-winding transformer model in PowerFactory is comprised of the 2-winding transformer element (ElmTr2), and the 2-winding transformer type (TypTr2). The transformer element allows input of data relating to the control of the transformer under steady-state conditions, and the transformer type allows input of the physical properties of the transformer.

Used as a WT transformer and WPP transformer

ElmZpu

The Common Impedance is a per unit impedance model including an ideal transformer. The main usage is for branches used for network reduction. The transformer ratio is equivalent to the nominal voltage of the connected busbars.

Used as a grid impedance

ElmLne

The ElmLne is an element used to represent transmission lines/cables. When referring to a type, the line element can be used to define single-circuit lines of any phase technology. In addition, the element parameter Number of Parallel Lines allows the representation of parallel lines without mutual coupling. For long transmission lines the distributed parameter model is preferred as it gives highly accurate results, while the lumped parameter model provides sufficient results for short lines.

Internal cable modeled as a lumped parameter element and cable between the PCC and Onshore bus modeled as a distributed parameter element

ElmShnt

The ElmShnt element is used to represent different shunt devices. The R-L shunt is a reactance/inductivity and a resistance in series.

Used as a reactive power compensation device

C Scientific Paper

Full-Scale Converter Wind Turbines in Weak Grids

Anna Golieva
European Wind Energy Master Student
Norwegian University of Science and Technology, Trondheim, Norway
Email: agoleva@gmail.com

***Abstract*—In the countries with long history of wind energy development and high penetration of wind power the latest grid codes appear to posses higher demands to the wind farms, now they have to comply with Low Voltage Ride-Through requirements, provide reactive power support to the grid, contribute to frequency and voltage control i.e., behave like a power plant [1]. Precisely it has been pointed out in [1]: Increasingly, wind farms will be required to provide the same system services as conventional power plants, for example inertia and possibly also black-start capabilities. DC links connecting synchronously operated areas can also be automatized to be used for primary power control.**

There is a strong tendency to locate wind farms in areas with best wind resources, which generally take place at remote and offshore locations. Therefore it is necessary to connect wind farm with long transmission lines, and in couple with weak grid the result is low Short Circuit Ratio connection of wind farms becoming frequent condition to deal with.

Foreseeing the prospectives of the newest generation of floating wind turbines development, which are no more limited by the sea depth, meaning the distance to the grid connection point will increase even more, resulting in longer lines and higher impedance between the wind farm and the grid. This paper investigates the behavior of full-scale converter wind turbine (Type 4) in weak grids, emphasizes the peculiarities of its modeling, steady-state simulations, analysis of occurring problems and overview of possible solutions.

***Index Terms* — Wind Generation, Low Short Circuit Ratio, Weak Grid, Voltage Source Converter**

I. Nomenclature

DC - Direct Current
DFIG - Doubly-Fed Induction Generator
GE - General Electric
LOS - Loss of Synchronism
LVRT - Low Voltage Ride-Through
PCC - Point of Common Coupling
SCR - Short Circuit Ratio
STATCOM - Static Compensation
SVC - Static VAr Compensation
VSC - Voltage Source Converter
VSWT - Variable Speed Wind Turbine
WPP - Wind Power Plant
WTG - Wind Turbine Generator

II. Introduction

The relevance of the problem investigated is conditioned by the recent updates in wind energy sector. The main purpose of the topic under consideration is connecting considerable amount of wind power generation to a weak grid, i.e., having Short Circuit Ratio lower than 2. The main features of the investigated case are high wind power penetration and connection through the long transmission lines. The ultimate goal of the study is to achieve good results, applying exclusively advanced control strategy without implying modifications to the grid topology.

III. Overview of the previous studies

Various research have been carried out on the topic, however the majority of them are focused on specific cases. For example, [2] is carrying out dynamic simulations of the voltage disturbance response of the WTG versus a conventional synchronous generator and presents relevant control design, however as it was stated by the authors, the model used was developed specifically for the GE 1.5 and 3.6 MW WTGs and the model is not designed for, or intended to be used as, a general purpose WTG. Therefore, substantial difference in the developed controller performance may occur when applying to a WTG of a different manufacturer and capacity. While [3] presents extensive study of the voltage stability issues occurring when a wind park of large capacity being connected to a weak grid. However the used grid model is not a generalized one, but on the contrary it fully represents a specific case of the ERCOT region grid in Texas.

Criteria of safe integration of large wind parks into weak grids have been studied in [6], whereas only induction machine based topologies have been investigated, namely types 1 (fixed speed squirrel cage induction generator) and 3 (variable speed wind turbine with doubly fed induction generator), though the new generation wind turbines possess essentially different behavior due to presence of a full converter, which eliminates the typical synchronous machine response effect on the system. Although [8] mentions a full converter turbine type, the study itself is focused on generator dynamic performance, which is not significantly relevant for the grid side of the full converter turbine type. An advanced control model against LOS event have been developed in [7], which is, however, tuned for the specific 70MW WPP project and verified by the tests on downscaled Micro-WPP, which doesn't guarantee the effective results when being applied to a wind farm of different topology.

In [4] it was discovered, that the fact, that WPP, unlike synchronous generator, is unable to increase the voltage in the weak grid during the fault. This is due to the fact, that while a synchronous generator is delivering high short circuit currents during faults, a WPP keeps its currents within nominal value.

The ultimate conclusion states, that voltage recovery with the WTG operating with controller proportional gain $K_p = 2$ and power ramp $P_{ramp} = 20\%$ is even slower, than in a case with no generation. That speaks for inadequacy of the requirements, stated in some grid codes and as it has been stated by the authors 'Simulations of a simple test system have shown that the minimum requirements set in some grid codes for voltage support of WPPs are inadequate and do not result in a satisfactory voltage recovery in weak grids. When reactive compensation is used to regulate the voltage in the weak grid, the voltage recovery with wind power installed may even be worse than in the case with no generation. However, it has been also stated, that full-scale converter WPPs have the capability to provide a post-fault voltage support comparable to the support provided by a synchronous generator of the same total capacity. In case of low X/R ratios, this requires a coordinated injection of the active and reactive current of the WPP during the fault, along with voltage support without deadband after fault clearing. The current injected by the WPP during the fault must have a $cos\phi$ dependant on the X/R ratio of the total network impedance as seen at the PCC. Moreover, it has been concluded, that a high proportional gain and a fast power ramp are also necessary to improve WPPs voltage support in a weak grid.' [4]

IV. Background of the investigated issue

First of all, the given studied situation posses general problems of grid with high wind power penetration. A system with wind power representing more, than 15% of total capacity is considered as a system with high penetration. According to [6], the wind power integration level is calculated as:

$$\rho = \frac{P_n}{S_{SC}} \tag{1}$$

where P_n is the nominal power of the wind farm and S_{SC} is the short circuit power of the grid. This parameter in certain way could also be referred to as an inverse of the short circuit ratio, which in its turn is expressed as:

$$SCR = \frac{S_{SC}}{P_n} \tag{2}$$

Though a certain clarification has to be emphasized: S_{SC} is a full power of a three-phase short circuit to ground, as seen at the PCC.

A. Weak Grid Concept

As it has been defined by [9], the 'strength' of the grid is determined by its impedance and mechanical inertia i.e., kinetic energy, stored in the rotating parts of the connected generators. Alternative representation, such as numerical value of the short circuit ratio is nothing more, than a comparison of the system power and power injection at the specified bus. It must be noted, that SCR is not a strength indicator of an entire system, but a measure of the system strength at the specified point, therefore a system, consisting of numerous generators and transmission lines will have different value of the SCR at each specific bus. In this paper further use of the SCR value will be always referred with respect to the PCC. Summarizing, application of SCR as a measure of grid strength is understood as an accepted approximation [9].

However, distinction must be made between the terms 'Weak Grid' and 'Grid with low SCR'. 'The SCR of a bus is an indication of the strength of the bus. The bus strength is defined here as the ability of the bus to maintain its voltage in response to reactive power variations. A system having high SCR will experience much less change in bus voltage than a network with low SCR. As it has been stated by [9], even though the SCR is calculated using steady state values, its value is a measure of how easily bus voltages are affected during dynamic system events.' [3]

In many cases, even when a wind park is being connected to a strong grid (i.e., low impedance grid or grid with high Short Circuit Power) via long transmission lines, which in their turn have high impedance, the resulting SCR seen at the PCC is being reduced and its value is primary determined by the line length. The issue being discussed further.

Weak Grids can be classified in four types:

1) Grid with low Short Circuit Power
2) Low SCR due to high grid impedance
3) Low SCR caused by connecting to low impedance grid through long cables
4) Grid internal fault resulting in increase of impedance and low SCR due to that

The findings of this work are mostly aiming to solve the problems, which occur at cases 2 and 3.

B. Voltage instability issues

Wind farms affects PCC voltage in a controversial way: they increase the voltage due to active power production and decreases it due to reactive power consumption. [1] 'Even though Type 4 wind farms are producing at unity power factor they consume reactive power for the transformers in wind farms and substations, and in the overhead lines. At the same time, wind farms feed active power into the grid. These two factors together reduce the power factor at the conventional power stations.' [1]

But the main concerns of the full converter concept are caused by the turbine behavior in response to grid faults, the issue being caused by low reactive power support capabilities. Even though the LVRT requirements demand that a wind turbine stays connected to the grid when a considerable voltage drop occurs, it is mostly resulting in WPP to maintain feeding active power into the grid, but the reactive power supply stays at the pre-fault level, which means - gives little contribution to the voltage recovery, compared to a conventional synchronous machine of the same capacity being connected to the same bus. The reason behind the difference is that a full converter, as it is typical for all power electronic appliances, possesses limited short circuit current capability. It is worth pointing out that in order to increase the reactive power supply necessary to recover the voltage, higher current injection is needed. That issues become particularly crucial on condition of weak grid, where $\frac{dV}{dQ}$ sensitivity is particularly high.

Furthermore, the situation is aggravated by the large portion of shunt capacitances in the lines impedances. As it is known, that reactive power, produced by the capacitors is directly proportional to the voltage squared, therefore in case of a voltage dip the injected reactive power decreases quadratically, whereas higher reactive power injection is needed for the voltage recovery, therefore the capacitor brings destabilizing effect in this case. [9] Due to that the effective short circuit ratio value is often used:

$$ESCR = \frac{S_{SC} - Q_c}{P_n} \tag{3}$$

where Q_c is the reactive power of all the shunt capacitances between a wind farm and a PCC.

C. Control related issues

The first logical solution of the voltage instability seems to be refine control strategy, while certain problems arise there. The latest findings state that a weak grid is causing faster response of the closed-loop voltage control, which in its turn leads to the oscillatory response, and in some cases fast response can also lead to temporary overvoltages, up to high voltage collapse [3], also in numerous cases the so-called 'good' SVC tuning in a weak grid results in faster response, but slows down recovery voltage and voltage oscillations [3].

'Some wind turbines (Type 3 and Type 4 in particular) have controls tuned for an SCR higher than some threshold (usually SCR>3). When the SCR is lower than this threshold value, the turbine control does not behave well, resulting in voltage oscillations.' [3].

It is known, that tuning of the controller gains is always a major issue, as it has to be designed on custom case basis. However the acute challenge is to develop a general high-level control logic that could be relevant for low SCR connected wind parks.

V. Simulations and findings

A. Wind Park Model and Characteristics

Even though DFIG (Type 3) wind turbines are still being used, it is not considered as a promising technology anymore. Therefore this paper deals with investigation of the problem for general purpose Wind Turbine Type 4 (full converter topology). First of all it should be noted that the fundamental peculiarity of type 4 WTG is that due to the presence of a full converter, which decouples the generator from the grid, its behavior is no more similar to the one of a synchronous machine, i.e., commonly referred to issues of angle stability, field voltage and synchronism are no more relevant. Therefore the full-converter wind power plant is usually being modeled as a voltage source behind an impedance [2].

This decision has great influence on simulation results: in conventional modeling, when a wind turbine is modeled as a synchronous generator, the turbine interacts with the network through an internal angle, which does not meet the reality in case when full converter is used, the further differences in model behavior are extensively investigated in [2].

The performance of the turbine is not affected by the change of grid frequency, as the generator frequency is tuned to optimize rotor speed [1]. Nevertheless it was proved, that not

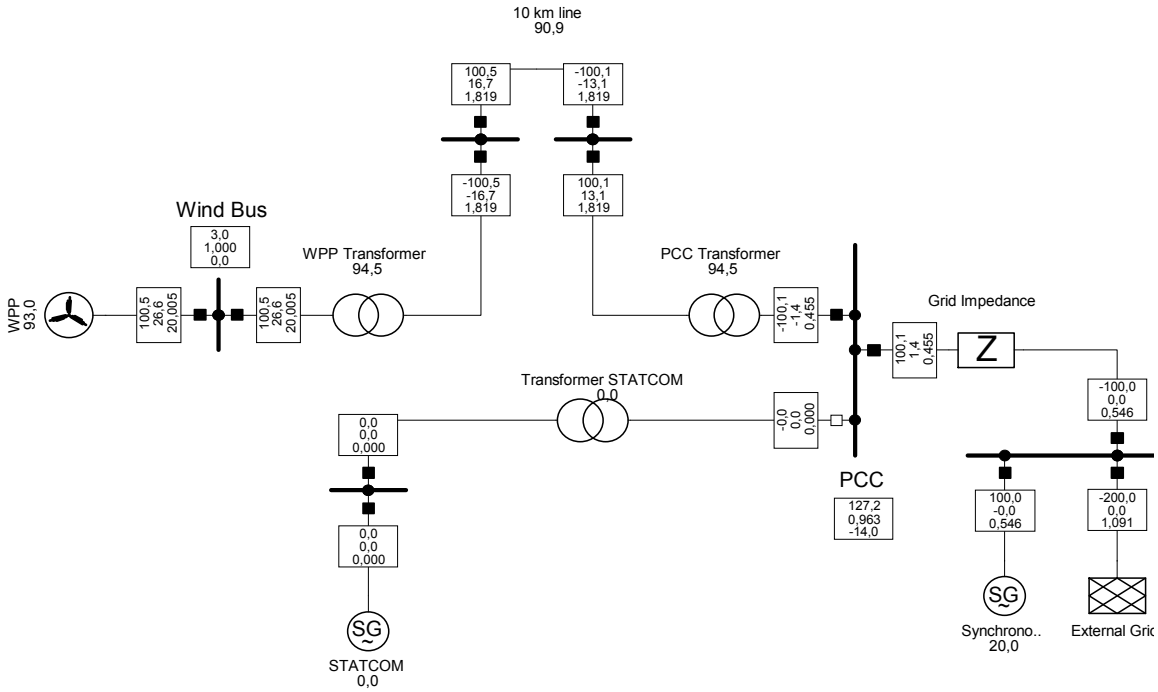

Fig. 1: Simplified model of the system in DIgSILENT Power Factory

only wind turbines have affect on the weak grid, but also a weak grid has certain effect on wind park behavior.

Even though the turbine is often represented as a voltage source behind an impedance and 'the fundamental frequency electrical dynamic performance of the WTG is completely dominated by the field converter' and 'the electrical behavior of the of the generator and converter is that of a current-regulated voltage source inverter' [2] the precise model should still posses certain properties of the conventional wind turbine model as its behavior is affected by factors, such as rotor inertia, blade pitching effects and intermittency due to effect of wind speed fluctuations. The latest require elaboration of the accurate wind model.

B. Software and modeling

For the preliminary simulation DIgSILENT Power Factory software has been selected as the preferred tool. For the steady state simulations the wind park is modeled as a lumped element wind turbine of 1p.u. capacity, connected to the external grid through a transmission line. STATCOM is used in order to compensate the reactive power, injected by the line. For the steady state studies STATCOM is being modeled as a synchronous machine with zero power factor, as it corresponds to the behavior of the actual STATCOM, namely - full controllability of injected reactive power, as demanded by the load flow solution. The main parameter of interest is the utility voltage, which is the voltage at the PCC in p.u. The decision has practical reasoning, as in many countries influence on the steady-state voltage is the main design criteria for the grid connection of wind turbines to the distribution grid. [1]. The layout of the system designed for the steady state studies is represented in figure 1.

The purpose of the preliminary studies is to determine, which factors have higher influence on voltage variations, i.e., higher sensitivity $\frac{dV}{dXX}$, where XX is the investigated parameter. The following investigated parameters have been selected: SCR and X/R ratio of the grid impedance.

C. Simulation results

Certain parameters have been varied in the steady state studies, in order to investigate the measure of the parameter change effect onto the steady state voltage at the PCC.

The distance from the wind farm to the PCC has been varied from 10 to 100 km, the line impedance being 0.033 Ohm/km. The X/R ratio is fixed at 10. Variable length of line and consequent change in line impedance cause changes in SCR. The simulation results can be observed at figure 2a, it has been proved that the lower is the SCR, the lower is the voltage at the PCC; and at a certain line length (approximately 70 km), when the SCR drops below 2, the utility voltage becomes less, than 0.95 p.u., which means it is below its admissible limits. The raw simulation data has been processed in order to obtain the voltage at the PCC dependence on the line length, i.e., impedance, which in its turn can be expressed as SCR.

Analogous simulations have been carried out for the different values of the X/R ratio, with certain modifications:

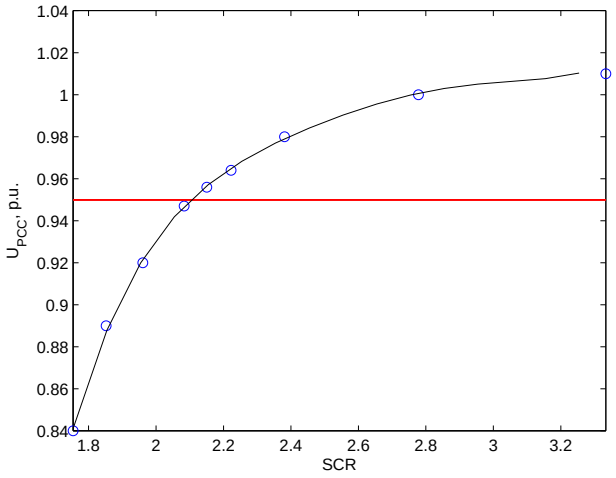

(a) Varied SCR.

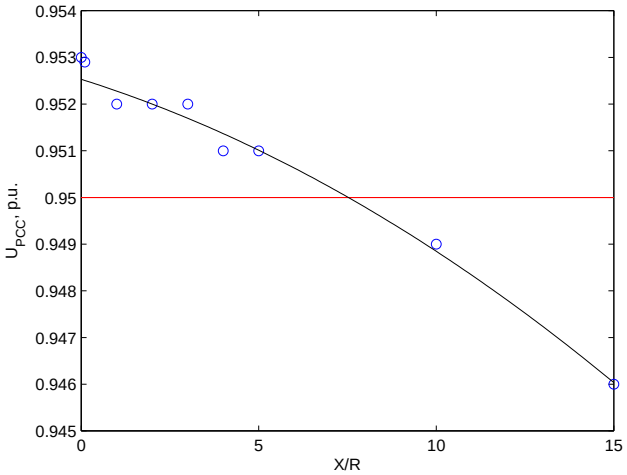

(b) Varied X/R ratio

Fig. 2: Voltage at the PCC as a function of the varied parameters.

line length has been fixed at 10 km, corresponding to the impedance value of 0.03p.u.; STATCOM has been disconnected from the PCC in order to prevent error due to over-compensation. The obtained results are shown in figure 2b.

The obtained functions have been differentiated in order to obtain dU/dXX sensitivities. The obtained results are shown in figure 3.

D. Proposed Voltage Stability Solutions

There are various possible solutions, mostly realized by means of power electronics, such as advanced tuning of the WT controller, WPP controller, application of synchronous condenser, SVC or STATCOM. Currently among the large variety of the power electronic solutions STATCOM seems to possess all the necessary qualities, complying with the grid codes, as it performs full controllability of reactive power

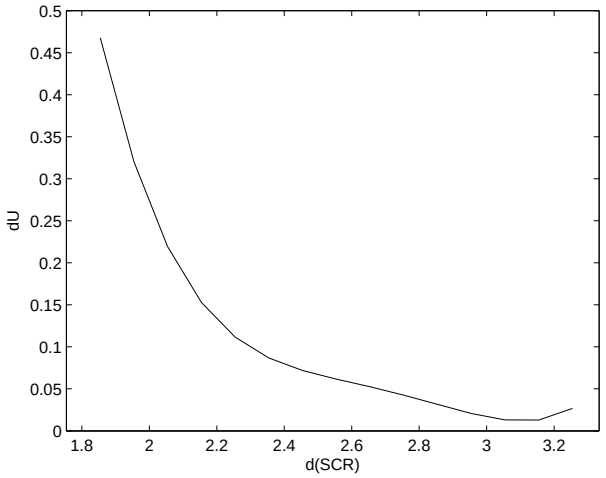

(a) $\frac{dU}{dSCR}$ sensitivity

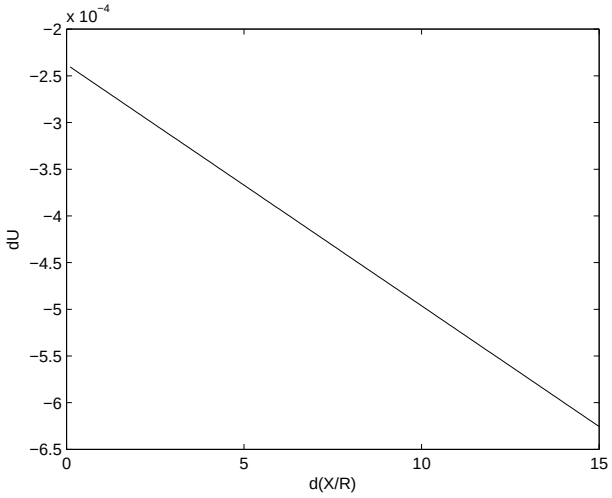

(b) $\frac{dU}{dX/R}$ sensitivity

Fig. 3: Approximated derivative of the voltage dependence on the varied factors $\frac{dU}{dXX}$

injection, but unlike synchronous condenser or SVC it shows good results in the voltage step size and speed of response.

VI. Conclusion

An attempt to generalize wind turbine behavior in weak grids has been taken and steady-state simulations have been carried out as they can in principle be used as simplified indicators of turbine dynamic behavior.

It has been concluded, that not all the discussed parameters have the same effect on the voltage deviation at the PCC. Namely it has been determined, that in the given case, the sensitivity $\frac{dU}{d(SCR)}$ is much higher, that $\frac{dU}{d(X/R)}$. While that is conditioned by the fact, that in the investigated case grid impedance is much smaller, than the impedance of connected lines, which is typical for cases 2 and 3, but might be different for cases 1 and 4. Therefore it can be seen that the ultimate goal for the further research on wind turbines connection to weak grids is elaboration of the general connection capability limitations, which would take into account all the weighted parameters, such as SCR, X/R ratio, penetration level, transmission capabilities, admissible voltage limits, etc. The objective is being complicated by the presence of the uncertainties, introduced by above-mentioned controller capability issues - controversial effect of proportional gains on the response speed versus stability. Also one of the topics demanding further research is the verification of the grid codes demands adequacy, both in terms of wind turbine protection and grid needs. Also as far as the widely used models of the wind turbines contain considerable amount of simplifications and assumptions, an important issue is the models validity verification in case of connection to networks with low SCR.

Acknowledgment

The author would like to thank all the master thesis supervisors for their patience and help.

References

[1] T. Ackermann, "Wind Power in Power Systems, 2nd Edition", Wiley, 2012.

[2] R. Piwko et al., "Integrating Large Wind Farms into Weak Power Grids with Long Transmission Lines", IEEE, 2006.

[3] S.-H. Huang et al., "Voltage control challenges on weak grids with high penetration of wind generation: ERCOT experience," Power & Energy Society General Meeting, 2012 IEEE, July 2012, pp.1,7.

[4] F. Sulla et al., "Wind turbines voltage support in weak grids," Power and Energy Society General Meeting (PES), 2013 IEEE, July 2013, pp.1,5.

[5] Y. Zhou et al., "Connecting wind power plant with weak grid - Challenges and solutions," Power & Energy Society General Meeting (PES), 2013 IEEE, July 2013, pp.1,7.

[6] R. Reginato et al., "Analysis of Safe Integration Criteria for Wind Power with Induction Generators Based Wind Turbines", IEEE, 2009.

[7] V. Diedrichs et al., Control of Wind Power Plants Utilizing Voltage Source Converter in High Impedance Grids, IEEE Power & Energy Soc. General Meeting, San Diego, California, USA, July 2012.

[8] J. W. Feltes and B. S. Fernandes, Wind Turbine Generator Dynamic Performance with Weak Transmission Grids, IEEE, 2012.

[9] A. Gavrilovic, "AC/DC System strength as indicated by short circuit ratios", in Int. Conference on AC and DC Power Transmission, London, UK, 1991.